Quantum Electronics **31** (2) 95 – 119 (2001)

REVIEW

PACS numbers: 42.60.Fc; 42.65.Re; 42.62.-b
DOI: 10.1070/QE2001v031n02ABEH001906

Ultrashort-pulse lasers

P G Kryukov

Contents

1. Introduction **96**
2. Historical overview **98**
3. Principle of mode locking **100**
3.1 Passive mode locking
3.2 Saturable absorbers for passive mode locking
4. Active media and pump sources **102**
5. Methods for measuring ultrashort pulses **104**
5.1 Intensity autocorrelator
5.2 Methods of frequency-resolved optical gating
6. Time coherence of radiation of femtosecond lasers **106**
6.1 Femtosecond laser as a comb-oscillator
6.2 Significance of the carrier-frequency phase of femtosecond pulses
7. Theoretical study of ultrashort-pulse generation **107**
7.1 Ultrashort-pulse formation in femtosecond lasers
7.2 Configuration of a Kerr-lens cavity
8. Kerr-lens femtosecond laser **109**
9. Amplification of ultrashort pulses **110**
9.1 Multipass scheme
9.2 Chirped pulse amplification
9.3 Diffraction-grating chirp controllers
9.4 The shortest high-power femtosecond pulses
10. Petawatt laser systems **112**
10.1 Hybrid Ti:sapphire/Nd:glass laser
10.2 Ti:sapphire laser
10.3 Generation of relativistic-intensity femtosecond pulses with the kilohertz repetition rate
11. Applications of ultrashort-pulse lasers **112**
11.1 Optical coherent tomography
11.2 Optical frequency standards
11.3 Precision material machining
11.4 Ultrahigh-intensity applications
12. Conclusions **116**
References

P G Kryukov Fiber Optics Research Center, General Physics Institute, Russian Academy of Sciences, ul. Vavilova 38, 117756 Moscow, Russia; P N Lebedev Physics Institute, Russian Academy of Sciences, Leninskii prosp. 53, 119991 Moscow, Russia;
e-mail: kryukov@fo.gpi.ac.ru

Received 24 February 2000; revision received 11 October 2000
Kvantovaya Elektronika **31** (2) 95 – 119 (2001)
Translated by M N Sapozhnikov

Abstract. **A review of the state of the art of ultrashort-pulse lasers is presented. Physical mechanisms of the formation of ultrashort pulses, methods for measuring their duration, and systems for their generation and amplification are considered. Some applications of femtosecond lasers in physics and chemistry, as well as in technology and medicine are discussed.**

Keywords: *ultrashort laser pulses, femtosecond lasers, applications of ultrashort-pulse lasers, measurements of parameters of ultrashort pulses*

1. Introduction

One of the most important problems of laser physics and quantum electronics is generation of extremely short laser pulses. The solution of this problem opens up the ways for building ultrahigh-power lasers. Such lasers allow one to achieve the energy concentration as high as that produced in the nuclear explosion. Another circumstance that stimulates the development of ultrashort-pulse lasers is the necessity of measuring extremely short time intervals in studies of various fast processes. The problem of time measuring itself includes the exact measurement of the current time, which is performed using the frequency standards, and the measurement of extremely short time intervals. Remarkably, the development of femtosecond lasers resulted in the outstanding achievements both in the field of measurements of extremely short time intervals and in the field of creation of laser frequency standards.

Since the advent of the first laser in 1960, a great progress has been achieved in the shortening of the laser pulse duration and increasing its power. Note that an increase in the laser pulse power is achieved in a great degree due to pulse shortening. The first laser of T Maiman generated an emission burst of duration of about 1 ms with the energy less than 1 J, this burst representing a random set of pulses of duration of about 1 μs. The peak power of this laser was ~ 1 kW.

Modern lasers are capable of emitting pulses of duration of about 5 fs, i.e., less than two periods of a light wave, which is close to the fundamental limit. Even comparatively modest laser radiation energy being concentrated in an ultrashort pulse will give high power, and upon a laser beam focusing, an enormous intensity. For example, the laser system built at Lawrence Livermore National Laboratory (USA) generates 440-fs pulses with the energy of 660 J, which provide the peak power exceeding 1 PW and the radiation intensity in the focused beam of 10^{21} W cm^{-2}. To have an idea of this magnitude, note that in this case the light pressure amounts to 300 Gbar, which is comparable with pressure inside the Sun!

The laser radiation power was mainly increased by shortening the pulse duration. Comparison of modern femtosecond lasers with the laser of Maiman shows that the increase in power achieves 12 orders of magnitude. To estimate the increase in the radiation energy, we can use the parameters of the National Ignition Facility being constructed in the USA for laser fusion studies. 192 beams of this huge facility the size of a football field will produce energy of 2 MJ in a nanosecond pulse. Thus, the increase in the energy will be no more than 6 orders of magnitude.

No less spectacular is the progress achieved in the efficiency and compactness of ultrashort-pulse lasers. Modern laser systems with the output power of tens terawatts can be installed on a tabletop. The development of injection semiconductor pump lasers, elements of fibre optics, and efficient SHG converters resulted in the building of extremely compact laser systems. Thus, IMRA (USA) reported the development of an extremely compact laser emitting 180-fs pulses with average power of 10 mW and a pulse repetition rate of 50 MHz, which fits on a palm!

A variety of applications of ultrashort-pulse lasers in fundamental science, technology, and medicine are based on the unique properties of their radiation. Extremely short laser pulses allow the study of ultrafast relaxation processes in microcosm, for which femtosecond is a natural time scale. Not without reason, the advent of femtosecond lasers is compared to the invention of a microscope. The enormous intensities in focused laser beams and the corresponding ultrahigh strengths of electric and magnetic fields allow one to study the interaction of light with matter in regimes that have been inaccessible so far for experimenters.

These lasers have been used to demonstrate the possibility of initiating nuclear reactions, to study some effects in quantum electrodynamics observed in the interaction of ultrashort laser pulses with ultrarelativistic electron beams, and to investigate a relativistic plasma. Methods have been developed for generating high-peak brightness X-ray and γ-ray radiation beams upon the interaction of ultrashort laser pulses with electron beams. The high-intensity pulses of duration less than 20 fs allow the generation of higher harmonic pulses of duration less than 100 as (an attosecond is 10^{-18} s) in the region up to soft X-rays.

Finally, the unique properties of the time coherence and the emission spectrum of femtosecond cw lasers have led to the revolutionary breakthrough in the field of precision frequency measurements in the optical range. In particular, the value of the fine-structure constant has been refined and the frequency of the $1S - 2S$ transition in the hydrogen atom has been measured with an accuracy of 1.8×10^{-14}. This opened up the possibility for creation of a more accurate optical clock.

In chemistry and photobiology, femtosecond lasers can be used to monitor ultrafast chemical reactions. Upon excitation of molecules by femtosecond pulses at various wavelengths with a variable delay between the pulses, photochemical reactions can be induced in certain channels, in which these reactions are unlikely to occur upon excitation by usual light sources. A new scientific field, femtochemictry, has appeared, and A Zevail has been awarded with the Noble Prize for his achievements in this field.

Considerable advances have been also achieved in technological applications of ultrashort-pulse lasers. Attempts to shorten the laser pulse duration naturally correspond to the tendency of modern electronics to miniaturisation and improving the fast response of electronic devices. Along with testing fast-response semiconductor circuits, femtosecond pulses can be used in future technologies, in particular, they can find applications in terabit fibre-optic communication.

The extremely high concentration of energy in focused beams from femtosecond lasers opens up a new way in the precision micromachining of materials and makes it possible to perform sophisticated operations in ophthalmology and neurosurgery.

The generation of ultrashort pulses has been considered in several monographs [1 – 4]. However, the progress in this field is so fast that many important results were not reflected in these works. In this review, the basic principles of generation of ultrashort pulses are reported and the most important results obtained in this field are described. Because of a limited size of the review, semiconductor and parametric ultrashort-pulse lasers are not considered here and applications of femtosecond lasers are illustrated only by the most spectacular modern results.

2. Historical overview

Since the discovery of the method for Q-switching of a laser cavity, which resulted in the increase in the peak output power by several orders of magnitude (giant pulse), another quite efficient method for the generation of ultrashort laser pulses – mode locking – was discovered almost at once. Unlike Q-switching, this method allows one to generate pulses that are much shorter than the round-trip time in the laser cavity. The method is based on the generation of many longitudinal modes with definite phase relations. The interference between generated modes produces beatings, and the time dependence of the radiation intensity represents a periodic train of pulses whose duration is inversely proportional to the width of the spectrum covering these modes and period is equal to the round-trip time in the cavity.

Such a generation regime can be obtained by introducing a light modulator into a laser cavity. The modulation frequency should be equal or multiple to the intermode frequency interval. Modulation at the intermode frequency results in the parametric enhancement of the adjacent modes with required phases, whose modulation enhances, in turn, the next adjacent modes, etc. This method of generation of ultrashort pulses was called active mode locking.

It was found soon that a periodic train of very short pulses can appear in the absence of a light modulator when a cell with a saturable dye intended for Q-switching was placed in a cavity of a ruby [6] or Nd : glass laser [7]. Because no modulation was required, this method was called passive mode locking. In this case, a giant pulse of a Q-switched laser represented an envelope of a train of very short pulses. The period of pulses in the train coincided with the round-trip time in the cavity, and it was obvious that the pulses appeared due to mode locking.

Measurements of the duration of these pulses with the help of fast-response photodetectors and oscilloscopes showed that it was shorter than the time resolution (about 1 ns) of the equipment used. For this reason, the methods for indirect measurements of the ultrashort-pulse duration were proposed and implemented, which were based on the detection of the autocorrelation intensity function using nonlinear optics phenomena such as SHG and two-photon fluorescence [8 – 10]. These methods showed that the duration of ultrashort pulses was several tens of picoseconds, which, in conjunction with Q-switching, gave an enormous peak power for the then existing lasers. A laser with an intracavity saturable absorber, Q-switching, and passive mode locking has become the *first-generation ultrashort-pulse laser*. Because of their simple design, these lasers have found very wide applications in science and technology, especially in nonlinear optics.

A similarity between the trains of ultrashort pulses in actively and passively mode-locked lasers suggested naturally that the formation of ultrashort pulses could be explained by the same mechanism [11]. It was assumed that beatings of two-three modes at the generation onset resulted in the formation of a pulse of duration of the order of the round-trip time in the cavity (axial period). This pulse, propagating through a saturable absorber, produces the amplitude self-modulation at the intermode frequency, i.e., it acts as an externally controlled modulator.

However, detailed studies of passively mode-locked lasers have demonstrated their substantial differences. The duration of ultrashort laser pulses was directly measured at P N Lebedev Physics Institute (Russia) with the help of an ultrafast image-converter streak camera with the time resolution of about several picoseconds [12]. The use of this technique showed [13 – 15] that the duration of individual ultrashort pulses could be about 10 ps, however, a rather complicated temporal structure of radiation was often observed, which could be varied during the train. It was found that groups of ultrashort pulses appeared during the generation, whose number, spacing, and the relative intensity could be varied within a broad range. This was obviously inconsistent with the mechanism of ultrashort-pulse generation in actively mode-locked lasers.

A considerable step in the establishment of the mechanism of ultrashort-pulse generation in passively mode-locked lasers has been made based on comprehensive studies of the propagation of short powerful laser pulses in amplifying and resonantly absorbing saturable media [16]. It was shown that, under certain conditions, not only the pulse shortening could occur but its temporal profile could also change, the most intense fluctuation peaks being predominantly amplified [17].

Direct streak-camera measurements showed that a two-component system consisting of an amplifying medium and a fast-response saturable absorber could strongly discriminate fluctuation pulses over their intensity [18]. Because a passively mode-locked laser represents a combination of an amplifying medium and a saturable absorber placed into the cavity, it was assumed that similar processes could be involved in the ultrashort-pulse generation.

In Ref. [19], a theoretical model of ultrashort-pulse formation in passively mode locked lasers was developed, which was based on the nonlinear mechanism of selection of the most intense fluctuation spikes in the temporal profile of the multimode radiation (the so-called fluctuation model). This model explained the experimental facts observed, namely, the necessity of removing from the cavity all the elements capable of selecting longitudinal modes and also the necessity of using a saturable absorber with a short (compared to the ultrashort pulse duration) relaxation time of the bleached state [20]. The studies aimed to the creation of saturable absorbers became an important aspect of the further development of lasers of this type.

The emergence of ultrashort pulses from fluctuation spikes was directly proved with the help of a streak camera [21]. Moreover, it was established that a passively mode-locked laser has two lasing thresholds. At the first threshold, free-running multimode lasing appeared and then, after a certain excess over the amplification, a train of ultrashort pulses was observed. An important role of the gain saturation and the ratio of the cross sections for the laser transition in the active medium and for absorption of the saturable absorber was also established. It was shown that this ratio could be controlled by placing a telescope inside the cavity between the active medium and a saturable absorber [22].

Detailed studies of ultrashort pulses at the initial part of the train and at the maximum of the envelope showed that ultrashort pulses change their shape during the development of the giant pulse [23, 24]. At the initial part of the train, a smooth bell-shaped pulse is observed, which acquires a complicated shape in the region of the envelope maximum: it represents an irregular sequence of components of durations shorter than the pulse duration at the initial part of the

train. Such a behaviour was explained by the effects of self-focusing and self-phase modulation [25].

The duration of ultrashort pulses generated by passively mode-locked solid-state lasers proved to be substantially greater than the limit determined by the gain bandwidth of the active medium. It was found that this was explained by a finite relaxation time of the bleached state of an absorber and by its substantial saturation at the final stage of the pulse evolution, resulting in a virtually complete ceasing of nonlinear shortening of the ultrashort-pulse duration.

The second generation of ultrashort-pulse lasers has appeared due to the discovery of organic dye lasers. A special feature of organic dyes is a very large gain bandwidth, which provides the tunability of the dye laser – the ability to smoothly vary the output wavelength over a broad spectral range. This feature made dye lasers an attractive object for studying generation of ultrashort pulses. Passive mode locking was obtained in a flashlamp-pumped rhodamine 6G dye laser with the DODCI dye used as a saturable absorber [26]. Then, the continuous operation of the dye laser was demonstrated which was pumped by light from an argon laser focused into the free jet of the flowing dye solution [27]. To compensate the astigmatism produced by the jet directed at the Brewster angle, the laser cavity had a special design.

An outstanding event in the development of ultrashort-pulse lasers was the achievement of passive mode locking in this cw dye laser with the help of a saturable absorber – the DODCI dye jet – placed into the cavity [28]. As a result, a continuous train of ultrashort pulses of duration of about 1 ps was generated. The pulse duration was later shortened to 0.5 ps [29].

Because the same components (rhodamine 6G and DODCI) were used in pulsed and cw lasers, it was assumed that the mechanism of the ultrashort-pulse formation should be also the same in these lasers. However, detailed studies of the pulsed laser with the help of a streak camera showed [30, 31] that the mechanism of the ultrashort-pulse formation in the dye laser is substantially different from that in the flashlamp-pumped solid-state laser. Thus, it was established that the discrimination of the fluctuation structure to a single ultrashort pulse on an axial period was com-pleted already within 20 – 30 round-trip transits in the cavity after the generation onset. This provided the quasi-continuous operation of the dye laser pumped by a flashlamp with the pulse duration of several microseconds.

The relaxation time of the bleached state of the DODCI dye was measured to be 225 ps, which is several hundred times longer than the ultrashort-pulse duration [32]. This apparent paradox, which could not be explained by the model of passively mode-locked solid-state lasers, was explained by the effect of a combined action of the amplification and absorption upon saturation [33]. The fact is that, unlike solid-state lasers, the cross section for the laser transitions in dyes is very large, being only several times lower than the absorption cross section. For this reason, Q-switching is absent, and the active medium and the absorber are saturated almost in the same degree. The leading edge of the pulse sharpens due to the absorber saturation, while its trailing edge sharpens because of saturation of the active medium.

A passively mode-locked cw dye laser became the main object of studies aimed at the shortening of ultrashort pulses. It is with the help of this laser that the breakthrough to the femtosecond region has been achieved. By using a ring laser, the optimal passive mode locking was provided in the so-called CPM laser (colliding-pulse mode-locked laser) [34]. As a result, the pulse duration did not exceed 100 fs. In the case of such short pulses, the group velocity dispersion (GVD) in the medium, through which the pulse propagates, becomes important. The pulse stretches and acquires the frequency modulation (chirp). By compensating this chirp in the CPM laser, the pulse was shortened to 53 fs [35].

The most important result achieved in the ultrashort-pulse generation was the invention of devices for changing GVD in a controllable way, which also allowed variation of the chirp in a broad range. These devices, which became the important component of laser systems for generation and amplification of femtosecond pulses, use either diffraction gratings [36] or prisms [37].

By using a prism compensator of GVD in the CPM laser, laser pulses of duration 27 fs were generated [38] due to optimal matching of the effects of self-phase modulation (SPM), GVD, and the saturation degree of dyes of the active medium and absorber. The stable operation of the laser was favoured by the appearance of a soliton-like propagation of ultrashort pulses in the cavity due to the combined action of SPM and GVD.

The ultrashort-pulse dye lasers reliably generate continuous trains of ultrashort pulses of duration of several tens of femtoseconds. Two lines of the development of ultrashort-pulse lasers have emerged. The first one is based on the use of flashlamp-pumped solid-state lasers, which generate high-power picosecond pulses. The second one employs comparatively low-power cw dye lasers, which generate, however, femtosecond pulses. The further progress of femtosecond lasers was related to the development of cw lasers systems pumped by lasers.

A significant stage in the development of solid-state ultrashort-pulse lasers was the fabrication of new solid laser media for generation ultrashort pulses. The so-called vibronic crystals have appeared, which exhibit broad absorption and gain bandwidths, such as $Ti^{3+} : Al_2O_3$ (sapphire) [39], $Cr^{3+} : LiCaAlF_6$ (LiCAF) [40], $Cr^{3+} : LiSrAlF_6$ (LiSAF) [40], $Cr^{3+} : LiSrGaF_6$ (LiSGaF) [41], $Cr^{4+} : Mg_2SiO_4$ (forsterite) [42], and $Cr^{4+} : YAG$ (black garnet) [43]. These crystals generated cw femtosecond pulses upon pumping by focused radiation from Ar and Kr lasers, Nd : YAG laser and its second harmonic, and single-mode semiconductor injection lasers (laser diodes). The use of vibronic crystal instead of dye solution jets has made femtosecond lasers by compact and reliable devices.

As was already mentioned, Q-switching in passively mode-locked pulsed solid-state lasers prevents the efficient pulse shortening because of the fast saturation of the absorber. To eliminate this drawback, schemes of the active [44] and passive [45] control of the feedback were invented. These schemes restricted the enhancement of the giant pulse and stretched the envelope of ultrashort pulses. However, even in the case of the feedback control, it was impossible to obtain femtosecond pulses because resonance saturable absorbers had picosecond relaxation times of the bleached state, which restricted the pulse duration. This stimulated the attempts to replace such an absorber by the device based on nonresonance optical nonlinearity [46].

The breakthrough in this field was achieved owing to a new laser design, where the main cavity was coupled with the additional cavity, where a medium with nonresonance

nonlinear susceptibility was placed. Single-mode fibres proved to be especially convenient for this purpose. The first implementation of this concept became a soliton laser [47], in which the nonlinear feedback from the optical fibre loop was coupled to the main cavity containing a synchronously pumped halide crystal with colour centres. In the absence of the additional feedback, pulses of duration of about 8 ps were generated. In the case of the optimal alignment of the additional cavity, the generated pulses were shorter than 200 fs. The formation of optical solitons in the fibre loop was substantial for the pulse shortening. Because this is only possible in the case of negative dispersion of the group velocity in the fibre, which is observed at $\lambda \geqslant 1.3$ μm, a KCl crystal with colour centres was used as an active medium operating at a wavelength of ~ 1.5 μm.

Then, it was proposed to use an additional cavity, without formation of solitons in it [48]. The passive mode locking was obtained by coherently adding a pulse with a shifted nonlinear, intensity-dependent phase, which was coming from an additional cavity, to the radiation in the main cavity. Such a method of passive mode locking was called additive pulse mode locking (APM) [49] or interference mode locking [50]. Its drawback is the necessity of aligning the length of the additional cavity with an interferometric accuracy. However, this drawback can be eliminated in cw lasers. The theory of the APM method is discussed in detail in Ref. [51].

Simultaneously with the development of the APM method, resonance saturable absorbers were improved. Using semiconductor layered structures (quantum wells), saturable absorbers were created, whose operating wavelength could be varied by choosing the proper materials and layer thickness. These devices were called semiconductor saturable absorber mirrors (SESAM) [52]. Unlike dyes, they have two relaxation times of the bleached state: a comparatively long relaxation time (tens of picoseconds), to which a lower saturation intensity corresponds, and a short relaxation time (tens of femtoseconds), to which a higher saturation intensity corresponds. This circumstance facilitates the initial discrimination of fluctuation peaks accompanied by the efficient shortening of a separated single ultrashort pulse.

A new method of passive mode locking was discovered in experiments with a Ti : sapphire laser [53]. It was found that self-focusing in a laser rod in conjunction with an aperture acted like a saturable absorber. Because the effect of self-focusing in a solid is based on the Kerr nonlinearity of the refractive index, it does not require resonance absorption and is virtually inertialless. This method was called Kerr-lens mode locking (KLM). Passively Kerr-lens mode-locked vibronic crystal lasers have become *the third generation of ultrashort-pulse lasers*. Their improvement resulted in the generation of ultrashort pulses of duration 5.4 fs (less than two periods of the light wave) [54].

Unlike lasers with saturable absorbers, in ultrashort-pulse lasers based on nonresonance nonlinearity, the self-start regime of mode locking can be absent, i.e., the initial discrimination of fluctuation peaks can be suppressed by the regenerative narrowing of the spectrum and (or) selection of the longitudinal modes. In this case, mode locking should be initiated by special means. For this purpose, one can use a saturable absorber with a low saturation level (for example, SESAM) [52], a piezoelectric drive of one of the mirrors with the feedback electronics, an amplitude modulator, as well as a mechanical push (snap on the cavity mirror or fast movement of one of the prisms of the GVD compensator) or synchronous pumping. Some of these devices are used for mode locking, in particular, a mode locker or an amplitude modulator controlled by an external oscillator. The question arises of whether it is pertinent in this case to speak about passive mode locking? According to the commonly accepted terminology, passive mode locking repre-sents the regime that is supported because of intracavity nonlinearities. The difference between active mode locking and passive mode locking with the additional start-up is that in the latter case the additional device can be in principle switched off after the development of the stationary regime, whereas in the former case the generation of ultrashort pulses ceases upon switching off the modulator.

Despite the excellent parameters of Kerr-lens femtosecond lasers, their considerable disadvantage is the high requirements imposed upon the pump laser. The pump laser should provide quite high and stable output power. Otherwise, the generation of a continuous train of femtosecond pulses will be interrupted even when a self-start device is used, which often increases the lasing threshold. These requirements increase the cost of femtosecond lasers, which is, as a rule, determined by the cost of pump lasers.

Studies of fibre-optic systems and diode-pumped solid-state lasers play a very important role in the solution of the problem of pumping. Because optical fibres can be doped with rare-earth ions, it is possible in principle to build a ultrashort-pulse fibre laser. Such lasers based on fibres doped with ions of Nd, Yb, and Er were demonstrated in Refs [55,56]. Studies of ultrashort-pulse fibre lasers resulted in the building of a simple and compact passive mode locking modulator based on the use of the nonlinear refractive index in conjunction with the cross modulation in media with weak birefringence [57]. Unlike a Kerr lens, the amplitude modulation required for passive mode locking was obtained in this case by adding a polariser rather than an aperture.

Diode-pumped femtosecond fibre lasers have become *ultrashort-pulse lasers of the fourth generation* [58, 59]. They are very compact, and the cost of pump lasers for them is an order of magnitude lower than that for Kerr-lens lasers.

The energy of a single femtosecond pulse does not usually exceed several nanojoules. Of course, it can be increased by transmitting the pulse through an active medium with the required gain bandwidth. To obtain a large amplification, the active medium should by sufficiently long. This is usually achieved with the help of a multipass scheme. To obtain a proper amplification, a much greater population inversion and, hence, the higher pump energy is required than for lasing. To achieve the required population inversion in the active medium of the amplifier, the pump pulse duration should be close to the relaxation time of the laser transition, which exceeds the period of ultrashort pulses in a train in the case of solid-state and excimer lasers. In addition, there exists a problem of heat removal. For this reason, individual ultrashort pulses being amplified are separated from the train using an electrooptical gate so that their repetition rate will be substantially lower.

The specific feature of the amplification of ultrashort pulses is that due to their extremely small duration, even comparatively low pulse energies (substantially lower than the saturation energy) cause nonlinear effects, which restrict the gain. The main of these effects is self-focusing.

To overcome this restriction, a new method for amplifying ultrashort pulses has been proposed, the so-called chirped pulse amplification (CPA) [60]. This method is an optical analogue of the method that is widely used in the radar technique. In this method, not the ultrashort pulse is amplified but the pulse that has the spectrum of the same width but stretched in time, its carrier frequency being varied linearly in time (chirped pulse). Since the power of this pulse is lower by a factor determined by the degree of its stretching, the role of restricting effects decreases accordingly and the pulse can be amplified up to large energies (up to the saturation energy). This is important for the efficient extraction of the energy stored in the active medium of the amplifier. After amplification, the pulse is transmitted through the delay line, in which the same time dependence of the carrier frequency is present, but with the opposite sign. As a result, the chirp is compensated and the pulse is shortened to its initial duration.

The CPA method provided peak pulse intensities of the order of terawatt in tabletop lasers in usual laboratories and even allowed the generation of petawatt ultrashort pulses [61, 62].

The CPA method was also successfully used for the further shortening of ultrashort pulses, for example, in the CPM dye laser [63]. The amplified 50-fs, 620-nm pulses were transmitted through a single-mode optical fibre of length several millimetres. In the fibre, a chirped pulse was formed owing the combined effect of SPM and GVD. The spectrum broadened, by covering almost the entire visible region. Then, this radiation was transmitted through a controller of GVD (including the third order), which consisted of prisms and diffraction gratings. Due to the chirp compensation, the pulse was shortened to 6 fs.

This result, which was obtained in 1987, was a record for a long time. A new modification of this method was demonstrated almost after ten years [64]. The amplified 140-fs, 660-μJ pulse from a Ti:sapphire laser was transmitted through a capillary with an inner diameter 140 μm and length 70 cm filled with inert gas (Ar or Kr) at a pressure of 4 atm, in which chirped pulses with the broadened spectrum were formed. After compression in a compensator consisting of a pair of prisms, a 10-fs pulse with the 240 μJ energy was produced. The improved setup with the use of chirp mirrors generated 4.5-fs pulses with the 15 μJ energy [65].

3. Principle of mode locking

According to the Fourier transform, a pulse of duration τ has the spectral width $\Delta\nu$ no less than τ^{-1}. Therefore, the necessary condition for the ultrashort-pulse generation is the use of an active medium with a sufficiently broad gain bandwidth. Because of a broad width of the lasing spectrum, the multimode lasing regime is naturally required. Two extreme cases of multimode lasing are possible. In the first case, the phases of electromagnetic waves of all modes are not coupled with each other, i.e., the phase differences of the adjacent modes are randomly distributed. In the second case, all the phases are coupled with each other in a certain way, i.e., the phase differences of the adjacent modes are the same, in other words, the modes are locked.

In the first case, the interference between modes results in the intensity variation in time in the form of a random series of fluctuation peaks in the time interval T, which is equal to the round-trip transit time for light in the laser cavity: $T = 2L/c$, where L is the optical path between the cavity mirrors and c is the speed of light (Fig. 1a). Upon successive transits between the cavity mirrors, this series of fluctuation pulses, which had characteristics of the thermal noise, is repeated with the period T, being amplified after each transit through the active medium.

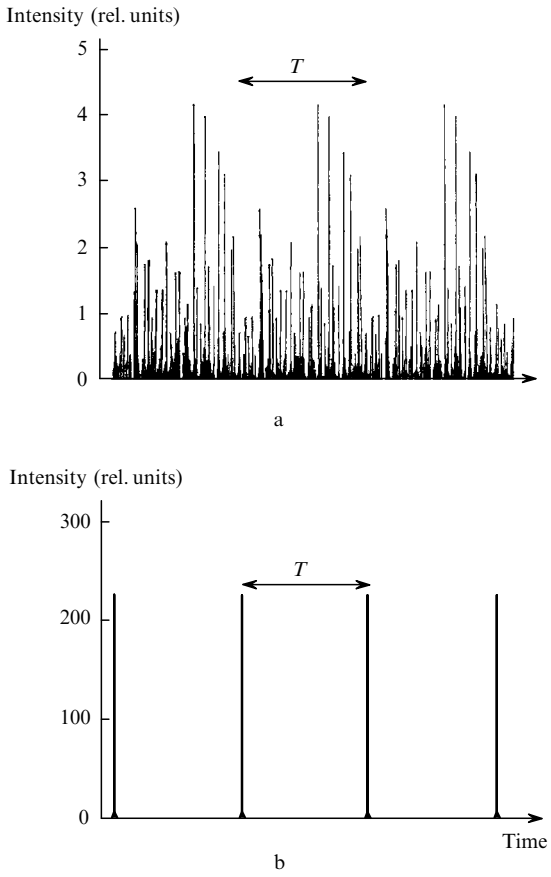

Figure 1. Time dependences of multimode radiation for random distributed modes (a) and for synchronised modes (b).

The average duration τ_f of an individual fluctuation peak is related to the width $\Delta\nu$ of the emission spectrum of the laser by the approximate expression $\tau_f \approx 1/\Delta\nu$. The width of the spectrum is determined by the number N of axial modes, which are spaced by the frequency interval $\delta\nu = 1/T$, i.e., $\Delta\nu = N\delta\nu$. This shows the principal possibility of the ultrashort-pulse generation. The multimode generation with a broad spectrum already contains ultrashort pulses. However, because of the random phase distribution, these pulses are randomly distributed over the entire period T and their intensity is low.

A completely different picture is observed in the second case, when the phase differences of adjacent modes have certain values. In this case, due to the interference, the emission energy of all modes is concentrated in a single pulse on the period T (Fig. 1b). The pulse duration τ is determined by the entire width of the spectrum and its intensity increases approximately by a factor of N compared to the first case. The operation of the ultrashort-pulse laser consists in essence in the providing of the regime at which many axial modes are generated, which are locked with each other in a certain way.

Generally speaking, one can imagine several scenarios of achieving such generation (Fig. 2). For example, as shown in Fig 2a, first the generation occurs at one mode. Then, the generation starts at two adjacent modes with the required phase difference and new modes appear in the vicinity of these two modes, which again have the required phase difference, this process proceeding until the filling of the entire gain band of the active medium. As a result, many modes with required phases are generated, which form a single ultrashort pulse on the axial period.

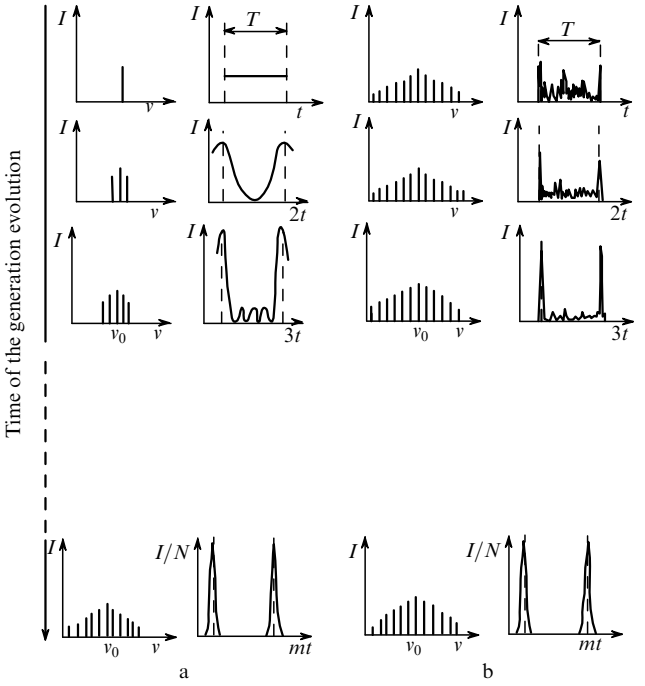

Figure 2. Scenario of the time evolution of generation of ultrashort pulses (in the number of round-trip transits in the cavity) in the cases when the generation starts at the central mode and then the adjacent modes with proper phases are generated (a) and when the generation starts simultaneously at all the modes with arbitrary phases and then the phases of all the modes change during the generation development (b).

According to another scenario (Fig. 2b), the generation starts simultaneously at all modes with arbitrary phases. In this case, as was mentioned, the radiation has a fluctuation nature. Then, the phase of each mode changes so that the phase difference of adjacent modes acquires the required value. A gradual variation of the phases is accompanied by an increase in the intensity of one of the fluctuation peaks and by a simultaneous decrease in the intensity of the rest of the peaks. In other words, the time profile of the radiation intensity circulating in the cavity changes. Fluctuation spikes of the radiation intensity become more and more rare, the intensity of one of them increasing much faster than that of the others, which begin then to reduce. Finally, an ideal picture of the generation of a single ultrashort pulse on the period T appears.

It should be emphasised that in both these scenarios, despite entirely different mechanism of mode locking, the final picture is the same – a single ultrashort pulse on the axial period. Therefore, the mechanism of mode locking cannot be determined from the final result. Historically, an actively mode-locked laser, in which ultrashort pulses are formed according to the first scenario, has been built at first [5]. Then, a passively mode-locked laser has appeared [6, 7]. The attempt has been made to explain the principle of its operation by the same mechanism of ultrashort pulse formation by considering the possibility of modulation of radiation in the cavity at the intermode frequency [11]. However, further studied showed that the operation of this laser is governed by the entirely different mechanism, which corresponds to the second scenario. One should bear this in mind, because there are encountered in the literature on ultrashort pulses incorrect explanations of the operation of passively mode-locked lasers based on the model corresponding to the first scenario.

3.1 Passive mode locking

To perform passive mode locking, it is important that the generation would start simultaneously at many modes with the fluctuation distribution of the radiation intensity in time that is characteristic for multimode radiation. In practice, this means that a passively mode-locked ultrashort-pulse laser has two thresholds. First, the generation of broadband multimode radiation appears and then, upon a further increase in the pump power, the generation of ultrashort pulses develops.

The time profile of the multimode laser radiation changes during its propagation through an active medium. The intensity of weak fluctuation pulses is reduced by a nonlinear absorber stronger than more intense pulses. Due to a combined action of the active (amplifying) medium and the nonlinear absorber, the fluctuation pulses experience a strong discrimination in their intensity. Finally, only a single ultrashort pulse remains in the cavity. It shape will change due to dispersion and nonlinear effects upon the interaction of laser radiation with a matter inside the cavity. Thus, one can conventionally distinguish two stages of the process: the formation of a single pulse from fluctuation pulses due to their nonlinear discrimination and final pulse shaping with the minimum duration.

The mechanism of ultrashort-pulse formation in a passively mode-locked laser is very sensitive with respect to the initial conditions of the laser operation. In principle, the generation can develop according to another scenario, when the spectrum will exhibit the regenerative narrowing, resulting in the broadening of fluctuation pulses until their complete smoothing. This is favoured by the conditions when one or several modes are predominantly amplified (have lower losses) compared to the rest modes. This leads to the well-known requirement of the careful removal from the cavity of any elements capable of discriminating longitudinal modes.

For this purpose, the faces of optical elements are aligned at Brewster's angle and mirror coating are deposited on wedge-like substrates. In principle, several spikes (with equal initial amplitudes) can be selected due to discrimination instead of one spike. In this case, several ultrashort pulses are generated on the axial period. An experimenter should provide the required regime by properly controlling the initial condition of the generation and by choosing the optimal laser design.

Note that, as a rule, there exists a rather narrow interval of the pump power in which the stable generation of single ultrashort pulses with the shortest duration is observed on the axial period. An increase in the pump power with the aim of increasing the peak power of ultrashort pulses often

results in the appearance of additional pulses on the axial period and in the increase in their duration.

3.2 Saturable absorbers for passive mode locking

The main element of a passively mode-locked laser is a saturable absorber, which reduces losses with increasing intensity of radiation propagating through it. The saturable absorber performs a rather fast self-amplitude modulation of losses in the cavity, whose degree depends on the radiation intensity propagating through the absorber. As a result, a 'window' of the positive gain appears on the time dependence of the total gain (the gain in the active medium minus losses in the cavity), which coincides with the intense pulse. The width of this window depends not only on the duration of the pulse formed but also on the relaxation times of the gain of the active medium and of the bleached state of the absorber. It is important to note that the role of the saturable absorber is twofold.

In the initial stage of generation, many windows are formed with the transmissions that depend on the intensity of fluctuation pulses. As a result, they are discriminated over the amplitude. The regenerative narrowing of the spectrum of multimode generation and, correspondingly, the smoothing of fluctuation peaks compete with this process. Once a single pulse has remained on the axial period, its shape changes upon successive passages through the window of the saturable absorber, i.e., weak peaks are suppressed in the initial stage, while the leading and trailing edges of the pulse are cut-off in the final stage. When the pulse becomes sufficiently short (less than picosecond), the GVD of the substance in the cavity and the self-action effects – self-focusing and self-phase modulation – become important.

Processes of discrimination of fluctuation pulses and final pulse shaping require, generally speaking, different characteristics of the saturable absorber. This is explained by the fact that the pulse intensities are substantially different in the initial and final stages of the ultrashort-pulse generation. It may happen that the saturable absorber will be capable of shortening a rather intense pulse but will be incapable of competing with the narrowing of the spectrum and of shaping single pulses on a period. This means that, since the laser with such an absorber cannot self-start, special means are required for increasing the degree of scatter over the fluctuation-peak intensities and, thereby, facilitating the formation of ultrashort pulses due to the intensity discrimination.

There exist various methods for the discriminating of fluctuation spikes. These are the methods that use a rapidly saturable absorber (dye or semiconductor) or a slowly saturable absorber (a combination of a slowly relaxing dye with the dynamic saturation of the active medium), the APM method, the Kerr-lens method, and the method of nonlinear optical rotation.

The three last methods are based on the nonresonance interaction of laser radiation with the matter, which leads to the dependence of the refractive index on the radiation intensity. There is no resonance absorption in these methods, which requires the consumption of the radiation energy. The transmission changes because of variation either in the wave phase and conditions of the interference (additional mode locking) or in the direction of beams (Kerr lens) or in the polarisation (nonlinear optical rotation). The refractive index of solids depends on the radiation intensity as $n = n_0 + n_2 I$. This phenomenon is known as the optical Kerr effect. The Kerr effect causes self-focusing and self-phase modulation, which play an extremely important role in femtosecond lasers. Because the refractive index changes due to the induced deformation of the electron cloud of an atom and this process occurs virtually instantly (for 10^{-15} s), these effects allow one to create an inertialless saturable absorber.

4. Active media and pump sources

Active media for generation of femtosecond pulses should meet the necessary requirement of having the gain bandwidth that is sufficient for producing pulses of a short duration. The second necessary condition is the high pump rate, which requires the high pump intensity. Such pumping can be achieved by focusing radiation from a cw laser into a sufficiently small spot. To do this, the pump laser should generate a single transverse mode at the wavelength lying within the absorption band of the active medium.

Femtosecond pulses have been first generated in organic dye solutions pumped by an argon laser. In these experiments, one of the dyes was used as an active medium and the other one as a saturable absorber.

At present, such solids as vibronic crystals and glasses doped with rare-earth ions are widely used as active media. An example of the vibronic crystal is sapphire doped with trivalent titanium ions (Ti^{3+}:Al_2O_3). The absorption band of this crystal is sufficiently broad and lies in the blue-green region, in which the emission wavelengths of an argon laser and of the second harmonic of a neodymium laser fall. The fluorescence spectra of some vibronic crystals doped with transition metal ions are shown in Fig. 3. The basic parameters of solids used in femtosecond lasers are presented in Table 1, where the parameters of the rhodamine 6G dye are also given for comparison.

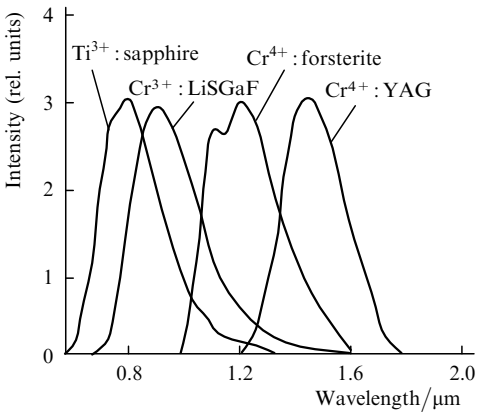

Figure 3. Fluorescence spectra of some vibronic crystals.

Note that glasses doped with rare-earth ions are widely used in femtosecond lasers. Elements made of glass can have virtually any size, and, which is especially important, single-mode glass fibres can be used for the building of compact femtosecond systems. The glass doped with Yb ions appears especially promising in this respect. The absorption and fluorescence spectra of this glass are shown in Fig. 4. One can see that these spectra are strongly overlapped. This means that the lasing and pump wavelengths are close to each other and, hence, this glass has the high quantum

Table 1. Spectroscopic and laser parameters of active media.

Medium	Pump band/nm	Gain line centre/nm	Gain line-width/THz	Cross section of the active transition/10^{-20} cm^2	Lifetime/μs	Pump source	Pump wavelength/nm
Rhodamine 6G	480 – 550	600	35	2×10^4	5×10^{-3}	Ar laser Second harmonic of a Nd : laser	514 530
Ti : sapphire	450 – 600	780	200	35	3.5	Ar laser Second harmonic of a Nd : laser	514 530
Cr:LiSAF	600 – 700	846	120	4.8	67	Kr laser GaInP diode	647 670
Cr:LiSGaAF	600 – 700	835	120	3.3	88	Kr laser GaInP-диод	647 670
Cr : forsterite	850 – 1150	1240	50	11	15	Nd : laser Nd, Yb fibre laser	1064 1060 – 1080
Nd : glass (phosphate)	~800	1055	8	4.2	350	AlGaAs diode	808
Yb : glass	~980	1040	50	~1	1000 – 2000	InGaAs diode	980

efficiency. Usually, pumping is performed by laser diodes at 980 nm and lasing is observed at $\lambda \simeq 1070$ nm, which yields the 92 % quantum efficiency and, correspondingly, a comparatively low heating. The high saturation energy (about 40 J cm^{-2}) makes this material very attractive for high-power amplifiers of femtosecond pulses.

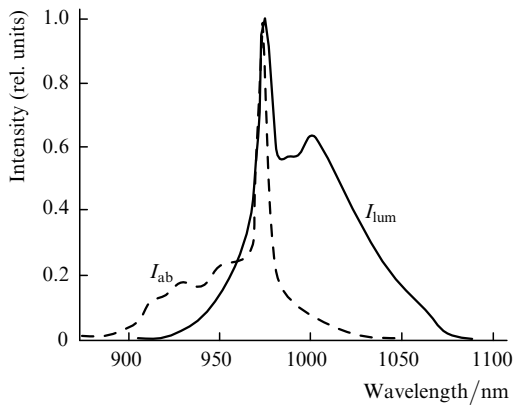

Figure 4. Absorption (I_{ab}) and fluorescence (I_{fl}) spectra of Yb : glass.

The use of semiconductor lasers, which possess the high efficiency, is of specific interest for the development of compact laser systems. These lasers can be directly used for pumping femtosecond lasers, if they provide the required cw power in the TEM_{01} mode. Laser diodes can be also used for efficient pumping solid-state cw lasers, whose single-mode radiation is used, in turn, to pump the femtosecond laser.

An example of such an approach is the use of diode arrays with intracavity SHG for pumping a Nd : YVO_4 laser. As a nonlinear element, the LBO or KTP crystals are commonly employed. In the development of femtosecond lasers, a special attention is paid to the generation of stable output power at the second-harmonic frequency because the noise of the pump source transfers to the train of ultrashort pulses. At present, laser systems emitting 5 W of cw power in the green region are manufactured by Spectra-Physics and Coherent.

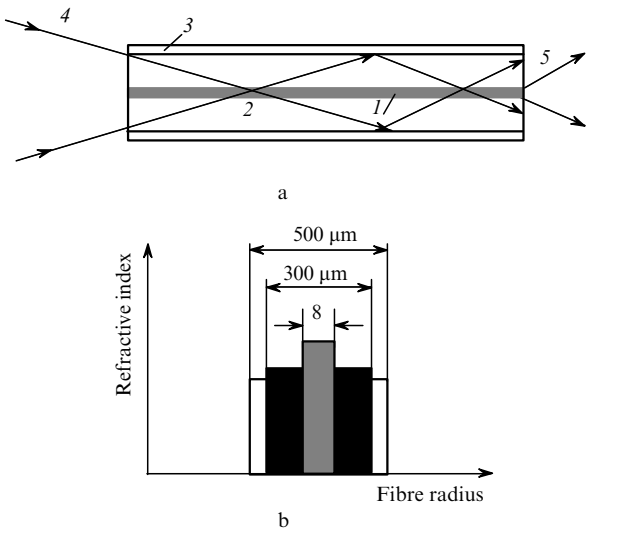

Figure 5. Schematic for pumping a single-mode active fibre through a cladding (a) and profile of its refractive index (b): (*1*) core (silica-glass fibre doped with rare-earth ions); (*2*) inner cladding; (*3*) outer cladding; (*4*) multimode pump radiation; (*5*) single-mode radiation from a fibre laser.

The second example, which illustrates the use of the diode array emitting multimode radiation, is the pumping of a single-mode fibre laser (Fig. 5). A core of the fibre forms a single-mode waveguide doped with rare-earth ions (Nd, Yb). Its diameter is commonly of about 8 μm. The inner cladding made of silica with a somewhat lower refractive index has a diameter of 200 – 300 μm. (Multimode radiation

of the diode array can be focused into a spot of this size). The fibre laser is pumped through this cladding. An external protective cladding made of a polymer material with a still lower refractive index provides the propagation of the multimode pump radiation through the fibre. The pump radiation repeatedly intersects the fibre core and is absorbed there by rare-earth ions. To enhance the efficiency of this process, the cross section of the inner cladding is made square or rectangular. Thus, the active fibre represents a peculiar converter of the multimode pump radiation to the single-mode radiation of the fibre laser. The output power above 3 W has been obtained in fibres doped with Nd [66] and Yb [67] ions with the efficiency of 50 and 63 %, respectively. The maximum output power of such systems at present amounts to 35 W. By using the pumped core, femtosecond fibre lasers can be also created [58, 59].

An important problem in the development of femtosecond lasers is the heat removal from an active element because these lasers operate in the cw regime. For this reason, it is preferable to use materials with the high heat conduction. A Ti:sapphire crystal, whose heat conduction is comparable with that of metals, is the best one in this respect. In fibre lasers, heat is released from a core to a fused silica cladding. Because the laser fibre is long, the heat flow in fibre lasers is lower than in lasers with usual rod active elements, while the volume of the external cladding is much greater than that of the core. For this reason, no special cooling is required for fibre lasers. In the amplifiers based on glass active elements, the repetition rate of ultrashort pulses should be usually lowered.

Femtosecond lasers operate in the visible and near-IR ranges, their gain bandwidths being so broad that they provide not only femtosecond pulses but also continious tuning of the emission wavelength in a rather broad spectral range. Because of the high peak power of femtosecond pulses, they can be efficiently converted to harmonics at the wavelengths falling within the gain bands of excimer lasers (308 nm for XeCL and 248 nm for KrF). Active media of excimer laser amplifiers have sufficiently broad bands, and the amplifier units can have a rather large size. This opens up the possibility for building high-power femtosecond lasers operating in the UV range [68 – 71].

5. Methods for measuring ultrashort pulses

To obtain the complete characteristic of the ultrashort pulse, one should measure not only its spectrum and energy but also its temporal profile. The first two procedures present no significant problems because the spectrum is rather broad. However, the measurement of the temporal profile of the ultrashort pulse is a complicated problem due to its extremely short duration.

Conventional time-resolved measurements with the help of photoelectronic devices such as photoelements, photodiodes, and photomultipliers in conjunction with the fastest oscilloscopes provide the time resolution that is several orders of magnitude less than the duration of ultrashort pulses generated by modern lasers. Even the best streak cameras prove to be obsolete for measurements of time intervals that are shorter than 100 fs. In this connection, the duration of femtosecond pulses is measured exclusively by optical methods that are based on correlation procedures. These methods permit one to measure not only the ultrashort pulse duration but also the time dependences of the amplitude and phase of the light wave with the subfemtosecond resolution.

5.1 Intensity autocorrelator

Information on the temporal parameters of ultrashort pulses can be obtained by measuring the autocorrelation intensity function. The autocorrelation function is usually measured with the help of the Michelson interferometer, which can provide the time delay τ between two interfering light beams. By varying the time delay, one can detect the dependence of the visibility (the ratio of the difference of the maximum and minimum of interference bands to their sum) on τ, i.e., to obtain the autocorrelation function of the light-wave field (the first-order autocorrelation function). This is a conventional application of the Michelson interferometer as a spectrometer.

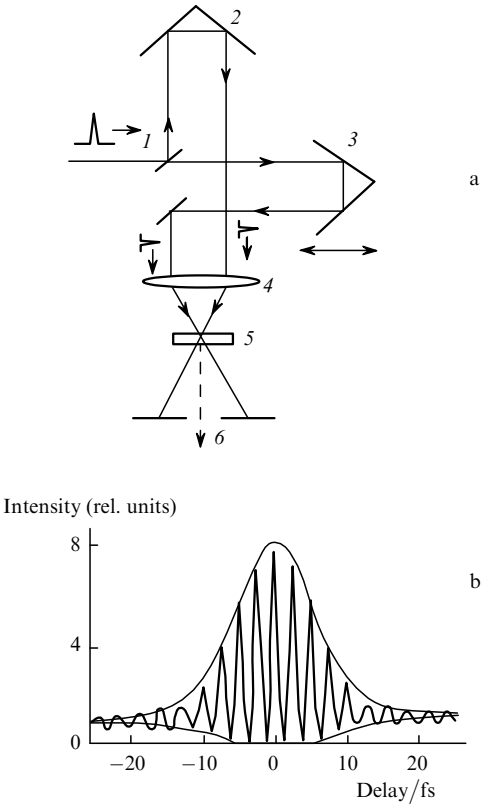

Figure 6. Principal schematic of the intensity autocorrelator (a) and the shape of autocorrelation function (b): (*1*) beamsplitter; (*2*) immobile reflector; (*3*) mobile reflector; (*4*) lens; (*5*) nonlinear crystal; (*6*) second-harmonic beam.

To measure the autocorrelation intensity function (the second-order autocorrelation function), the output radiation of the interferometer is directed to an intensity-nonlinear element. For this purpose, a nonlinear crystal is commonly used, which converts the incident radiation to the second harmonic. By detecting the dependence of the second harmonic radiation on τ, one obtains the autocorrelation intensity function

$$G^{(2)}(\tau) = \int \left\{ [I(t) + I(t+\tau)]^2 \right\}^2 \mathrm{d}t, \qquad (5.1)$$

where $I(t)$ is the intensity of radiation incident on the crys-

tal. The integration corresponds to the averaging and accumulation of the detected signal.

Two schemes of the correlator are possible. The first scheme (Fig. 6a) uses the noncollinear (vector) synchronism, when the output beams are focused on a thin nonlinear crystal so that the angle between them would correspond to the vector synchronism condition. In this case, SHG occurs along the bisectrix of this angle. The necessary condition for SHG is the temporal overlap of the interfering pulses. In this case, the autocorrelation function has the bell-like shape with the zero background.

In the second scheme, both output beams are mutually overlapped and the collinear synchronism takes place in the nonlinear crystal. In this case, the autocorrelation function has a background and represents the interference peaks with a bell-shaped envelope (Fig. 6b). For the transform-limited pulses, the ratio of the maximum interference peak intensity to that of the background (contrast) is 8:1. The contrast value allows one to judge the presence of transform-limited pulses, while the interference pattern itself can be used for calibrating the autocorrelator. If a semiconductor diode is employed as a detector, a nonlinear crystal is not required [72]. The photodiode material should have the energy gap that exceeds the photon energy. In this case, both the nonlinear process and its detection take place.

Table 2 presents the relations between the pulse duration and the width of the autocorrelation function for pulses of different shapes.

Table 2. Relations between the pulse duration Δt, the width $\Delta\tau$ of the autocorrelation function, and the width $\Delta\nu$ of the spectrum for pulses of the different shape.

Pulse shape	$I(t)$	$\Delta\tau/\Delta t$	$\Delta t\,\Delta\nu$
Gaussian	$\exp\left[-2.77(t/\Delta t)^2\right]$	1.414	0.44
Sech^2	$\mathrm{sech}^2(1.76t/\Delta t)$	1.543	0.315

The theory of ultrashort-pulse generation predicts that the pulse shape is described by the function sech^2. In this case, upon complete mode locking, the ratio of the pulse duration Δt to the width of the autocorrelation function $\Delta\tau$ is $\Delta\tau/\Delta t = 1.54$, and the product of the pulse duration by the width of the spectrum is $\Delta t\,\Delta\nu = 0.315$. The obtaining of this value for ultrashort pulses is usually treated as the achievement of complete mode locking.

5.2 Methods of frequency-resolved optical gating

Measurements of the autocorrelation intensity function do not give complete information on the ultrashort pulse. In particular, if the pulse contains the chirp (sweep of the carrier frequency), it can be detected with the help of the above-described methods, but its sign cannot be determined.

To determine the pulse shape completely, one should know its amplitude $A(t)$ and phase $\varphi(t)$. These quantities are determined, generally speaking, by using two different methods – the temporal and frequency ones. In the case of the temporal method, the measurements are performed that allow one to determine the moment of appearance of the given frequency in the specified time interval (gate). For this purpose, the method of frequency-resolved optical gating (FROG) is used. In the case of the frequency method, the moment of appearance of the given frequency component is measured.

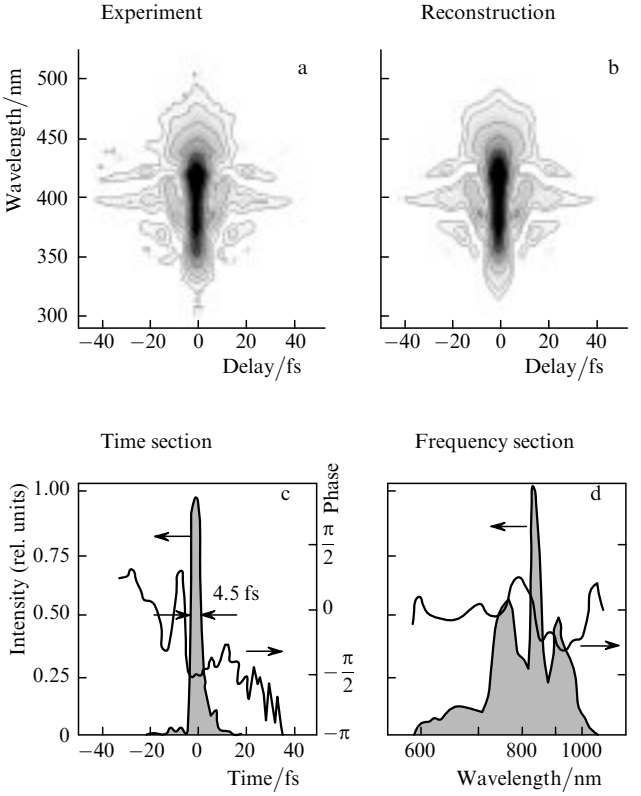

Figure 7. Example of detection of a 4.5-fs pulse [75].

In both these methods, spectral measurements are based on the cross-correlation. The cross-correlation can be obtained by using either the third-order susceptibility $\chi^{(3)}$ (the optical Kerr effect) or, more often, SHG [73, 74]. In the latter case, the pulse being measured is split into two beams, one of them being delayed with the time delay τ_r. Having crossed in the nonlinear medium, the beams give the same signal as in the autocorrelator, which then decomposed into a spectrum.

The results of the measurements can be represented as a three-dimensional plot of the function

$$I_{\mathrm{FROG}}(\omega,\tau_r) = \left|\int E(t,\tau_r)\exp(\mathrm{i}\omega t)\mathrm{d}t\right|^2. \qquad (5.2)$$

An example of the study of the ultrashort pulse of duration 4.5 fs is shown in Fig. 7 [75].

The frequency method has been implemented by using different procedures of the reconstruction of the pulse shape with the help of interferometry of frequency-shifted pulses [76, 77]. One of them is the spectral phase interferometry for direct electric-field reconstruction (SPIDER) [78]. In this method, one of the parts of the split pulse is transmitted through a delay line with the group velocity dispersion, which produces the pulse with the specified chirp involved in the nonlinear process. This method gives complete information for one pulse [79].

6. Time coherence of radiation of femtosecond lasers

Continuously operated femtosecond lasers exhibit quite unusual properties of the time coherence of radiation. As is known, the coherence is the concordance between oscillations in the electromagnetic wave of a light beam. Usually, the coherence is manifested as an ability of the light beams to produce interference, so that interferometers are classical devices for measuring the degree of coherence. The Young interferometer is used for measuring the spatial coherence, while the Michelson interferometer is employed for measuring the time coherence. It is accepted that the time cohe-rence is equivalent to the monochromaticity of light. Because the emission spectrum of ultrashort pulses is broad, it seems at first glance that the time coherence of this emission is low.

However, in the case of a periodic train of pulses, the situation can be different. If the pulses are identical and their repetition rate is strictly constant, the concordance between oscillations in the electromagnetic wave in pulses will persist as long as is wished. When such radiation is studied with the Michelson interferometer, the interference pattern will be periodically repeated due to the interference of the preceding pulse with each of the subsequent pulses. Mathematically, this is quite obvious: a periodic train of pulses is described by a Fourier series with equidistantly spaced sinusoids (frequencies), in contrast to a single pulse, which is described by a Fourier integral with the continuous spectrum.

The cw femtosecond laser emits a periodic train of pulses, whose frequency is sustained with a high-Q cavity. Therefore, the emission spectrum of the laser represents an equidistant sequence of narrow lines filling the width of the spectrum.

Consider a typical experimental situation when a single pulse is separated from a continuous train, for example, for the further amplification. This can be accomplished using a fast electrooptical gate. After the gate, the pulse shape does not virtually change, whereas its spectrum changes dramatically. Before the gate, the spectrum of the pulse consists of the equidistant narrow lines whose envelope has the width determined by the pulse duration. After the gate, the spectrum becomes continuous and coincides with this envelope. The emission at a single mode can be separated from the emission of the cw femtosecond laser with the help of a monochromator. In this case, the time dependence of the emission intensity changes dramatically. Before the monochromator, this dependence represented a periodic train of ultrashort pulses, whereas, after the monochromator, emission with the constant intensity is observed. Therefore, the time coherence of a cw ultrashort-pulse laser should be characterised by the two times. The minimum time is determined by the ultrashort pulse duration, while the maximum time is determined by the train stability. Note that the latter time can greatly exceed the train period. Of course, one can separate a group of pulses using the gate, i.e., to interrupt the train and to obtain the intermediate value of the time coherence.

Indeed, the same Ti:sapphire femtosecond laser has been used both in the optical coherent tomography [80] (as a light source with an extremely low time coherence) and for precision measurements of optical frequencies [81], which require a very high time coherence.

6.1 Femtosecond laser as a comb-oscillator

Radiation of a mode-locked cw laser exhibits a comb of equidistant frequencies of the constant intensity. An oscillator emitting such a comb of frequencies is called a comb-oscillator. A cw femtosecond laser that can be used as a comb-oscillator operating in the visible range allows one to solve efficiently the problem of the absolute measurements of the optical frequency [81].

Note another application of the ultrashort-pulse laser as a comb-oscillator. In contemporary systems of fibre optic communication, the technique of combining and separation of optical signals over the wavelengths of carrier frequencies is used. This strongly increases the bit rate of a communication channel. The cw ultrashort-pulse laser provides a sufficient number of channels separated over the wavelengths. Using a dispersion system (prisms, diffraction gratings, filters), the output radiation can be spatially separated into several beams, which corresponds to different frequency components. The beam intensity (which is constant for each of the beams) can be modulated with the broadening of the spectrum within the frequency interval between the modes. Then, the beams should be again combined to form a single beam with the help of a similar dispersion system. The frequency interval between channels is controlled by the cavity length, and the total width of the channel band is determined by the pulse duration. Of course, compact and highly efficient fibre or semiconductor ultrashort-pulse lasers are appropriate for use for this purpose. The bit rate of the order of 1 Tbit s^{-1} achieved by this method has already been demonstrated [82, 83].

Note that, if the pulse duration proves to be greater than that requires for the total bandwidth, the comb of equidistant frequencies can be extended by using the generation of continuum in a fibre with a photonic-crystal microstructure, as in the application of femtosecond lasers in precision frequency metrology [84].

6.2 Significance of the carrier-frequency phase of femtosecond pulses

Radiation of a cw ultrashort-pulse laser is characterised by the carrier frequency ω_0 at the centre of the gain band of the active medium, which is modulated by pulses with the repetition rate f_r whose shape is described by the amplitude envelope $a(t)$. The pulse repetition rate is determined by the round-trip transit time for light in the cavity. It can be

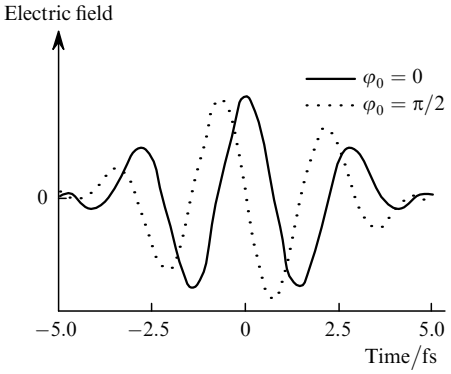

Figure 8. Time dependences of the electric field of the light wave for a 5-fs pulse at 750 nm with different phase shifts between the carrier frequency and the envelope maximum.

easily measured and controlled by moving one of the mirrors. In the general case, the carrier frequency can be shifted by φ with respect to the maximum of the envelope. Then, the electric field of the light wave can be represented in the form

$$E(t) = a(t)\cos(\omega_0 t + \varphi). \tag{6.1}$$

When the pulse duration approaches the carrier period, the time dependence of the electric field is substantially determined by the phase value. Fig. 8 shows two such dependences for pulses of the same shape and duration (5 fs) but with the different phase shifts between the maximum of the envelope and the carrier frequency ($\lambda = 750$ nm) [85]. One can see that these dependences are different. This circumstance was revealed when the pulse duration was close to 10 fs because this dependence substantially affects nonlinear effects, in particular, the generation of high harmonics [86]. This situation is discussed in more detail in Section 11 devoted to applications of ultrashort-pulse lasers.

The methods for measuring the phase shift between the envelope and carrier frequency based on the use of nonlinear effects, such as SHG and the generation of the difference and sum frequencies, have been proposed and studied in Refs [87, 88]. The phase shift between the carrier frequency and the envelope is manifested in the frequency domain as the frequency shift of the frequency comb of the comb-oscillator, so that it was measured by the methods of precision metrology of optical frequencies.

7. Theoretical study of ultrashort-pulse generation

The basic problem of the theory of femtosecond pulses is the elucidation of the question about the shortest pulse duration that can be obtained under controllable experimental conditions. Another no less important problem is how to provide the conditions under which the nonlinear effects (for example, related to the Kerr lens) would cause stable passive mode locking, resulting in the generation of pulses of the shortest duration. It is very important to find out whether the self-starting regime is possible and at what expense, i.e., whether it would not result in the substantial deterioration of the output parameters.

7.1 Ultrashort-pulse formation in femtosecond lasers

As already mentioned, the ultrashort-pulse generation in passively mode-locked lasers can be conventionally divided into two stages. At the first stage, the gain window produced by a nonlinear element performs the discrimination selection of an intense peak from the fluctuation structure of the multimode radiation of the free-running laser. Then, the separated single pulse acquires the final stationary shape after repeated transits through the intracavity elements. The ultrashort-pulse formation due to the Kerr-lens self-amplitude modulation (SAM) has been theoretically studied in a number of papers [51, 89, 90].

Analytic studies have been based on the assumption that the pulse suffers a small fractional change in phase and amplitude when passing through the cavity elements during its circulation in the cavity. This assumption is valid for the cw operation. It is also assumed that the gain relaxation time is much greater than the round-trip transit time in the cavity, while the pump level is kept constant.

The electric field of the light wave of a single pulse formed at the end of the first stage of the transient process can be written in the form

$$E(t) = a(t)\exp(\mathrm{i}\omega t). \tag{7.1}$$

Pulse shaping upon passage through any one of the cavity elements is described by

$$\frac{\partial a}{\partial z} = \hat{P}a, \tag{7.2}$$

where z is the space coordinate along the propagation direction and $\hat{P}$ is the propagation operator. The complex envelope of the output pulse is related to that of the input pulse by

$$a_{\mathrm{out}} = \exp(\hat{P})a_{\mathrm{in}}. \tag{7.3}$$

The operator $\hat{T}$ describing a full round-trip in the cavity is obtained by multiplying the operators of each element in the order of their action in the cavity. Note that, generally speaking, the action of the operators on the pulse depends on the element position in the cavity and on the direction of pulse propagation. Taking this into account, the pulse evolution at the point z after the nth round-trip transit is described by the equation

$$a_{n+1}(t, z) = \hat{T}(z)a_n(t, z). \tag{7.4}$$

The steady state is reached when

$$a_{n+1}(t, z) = \exp(\mathrm{i}\psi)a_n(t, z), \tag{7.5}$$

where $\psi = \psi(T)$ is a slowly varying phase shift.

This formalism has been applied for the description of solid-state femtosecond lasers [89, 90]. Fig. 9 shows schematically the arrangement of the elements in the cavity and the action of operators

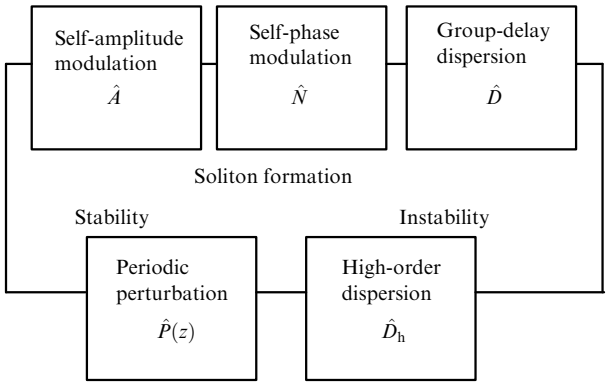

Figure 9. Schematic of the arrangement of elements in the cavity and functions of the corresponding operators.

$$\hat{P}_1 = \hat{D} = \mathrm{i}\frac{D}{2}\frac{\partial^2}{\partial t^2},\ \hat{P}_2 = \hat{A} = \frac{1}{2}\left(g - l - k|a|^2\right),$$

$$\hat{P}_3 = \hat{N} = -\mathrm{i}\phi|a|^2, \tag{7.6}$$

where D is the GVD; g and l are the gain and loss; k is the coefficient of nonlinear amplitude modulation; ϕ is the coefficient of SPM. A specific feature of a Kerr-lens femtosecond laser is that SPM ($\phi \sim 10^{-6}$ W^{-1}) exceeds the Kerr-lens amplitude modulation ($k \sim 10^{-7}$ W^{-1}). As a result, the pulse shortening is predominantly caused by the combined action of the negative GVD and positive SPM, while the passive modulation facilitates the formation of a single ultrashort pulse and provides the stable operation of the laser. In the limit $k/\phi \to 0$, a nonlinear Schrödinger equation is obtained whose solutions have the form

$$a_n(t) = (W/2\tau_\mathrm{s})^{1/2}\mathrm{sech}(t/\tau_\mathrm{s})\exp(\mathrm{i}\phi_n), \tag{7.7}$$

$$\phi_n = \phi_0 + nD/\tau_\mathrm{s}^2, \tag{7.8}$$

$$\tau_\mathrm{s} = 2D/\phi W, \tag{7.9}$$

where W is the pulse energy and τ_s is its full width at half maximum. Equations (7.7)–(7.9) describe the pulse that is identical to a fundamental soliton propagating in a nonlinear optical fibre with negative GVD [57].

In practice, the only parameter of the smooth variation of the ultrashort-pulse duration is GVD. If $D > 0$, the combined action of SPM and GVD results in the pulse broadening. Conversely, the combination of negative GVD with SPM results in the efficient shortening of the pulse and a soliton-like regime emerges. It follows from Eqn. (7.9) that, if $D \to 0$, the ultrashort pulse will have zero duration, which, of course, has no physical meaning. This is explained by the fact that Eqn. (7.9) was obtained assuming that the gain bandwidth is infinite. To take the gain bandwidth into account, the operators are introduced that describe the high-order dispersion, the perturbation along the pulse propagation coordinate, and other processes [89]. In this case, only numerical solutions can be obtained, which predict

$$\tau_\mathrm{s} = 3.53|D|/\psi W + \alpha\psi W, \tag{7.10}$$

where a proportionality factor is $\alpha \approx 0.1$ from the side of the mirror with the GVD compensator and ~ 0.25 at the opposite end.

The third-order dispersion (TOD) D_3 begins to play a noticeable role when a change in the second-order dispersion over the entire spectrum of the pulse becomes comparable with the dispersion itself. The numerical solutions [90] give the criterion of the stable generation of transform-limited pulses:

$$|D_3| < 0.2|D|\tau. \tag{7.11}$$

The control of the TOD becomes necessary for the generation of pulses shorter than 10 fs.

7.2 Configuration of a Kerr-lens cavity

The action of an artificial nonlinear absorber consisting of a Kerr lens in conjunction with an aperture is rather weak. For this reason, to obtain the maximum SAM and to produce stable mode locking, a cavity of a special design is required. The parameters of such a cavity were calculated in Refs [91–93], where Gaussian beams were analysed using the ABCD matrix formalism. The aim of the analysis was to find the exact positions of mirrors and the active element. A special feature of the schemes under study is that to produce the required intensity level, the pump beam is focused by a short-focus lens and the active medium is placed between two confocal adjacent concave mirrors. To reduce losses, the ends of the active element are cut at Brewster's angle, resulting in a significant astigmatism, which is compensated by the beam tilt [27].

The equivalent schematic of the cavity is shown in Fig. 10. Focusing mirrors (represented by lenses with focal distances f_1 and f_2) forms a mode on the cavity with a small cross section of the caustic of the active medium (d_1/f_1 and $d_2/f_2 \gg 1$). A small diameter of the beam in the active medium is required for producing the high intensity needed for the operation of the Kerr-lens mechanism. To maintain a stable Gaussian TEM$_{00}$ mode in the four-cavity mirror with $f_1 = f_2 = f$, the optical distance d between the focusing mirrors should somewhat exceed $2f$, i.e., it should be $2f + \Delta$. The regions of the values of Δ at which the cavity is stable are determined by the relations

$$0 < \Delta < \Delta_1,\ \Delta_2 < \Delta < \Delta_\mathrm{max}, \tag{7.12}$$

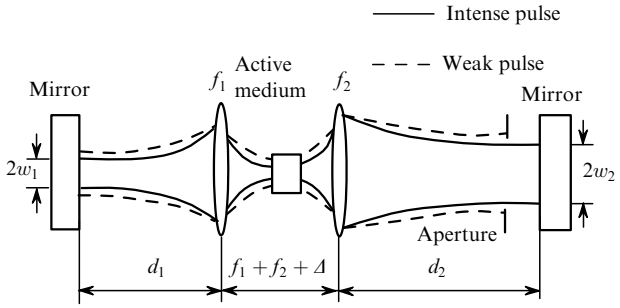

Figure 10. Equivalent schematic of the Kerr-lens laser cavity.

where

$$\Delta_1 = f^2/(d_1 - f);\ \Delta_2 = f^2/(d_2 - f);\ \Delta_\mathrm{max} = \Delta_1 + \Delta_2. \tag{7.13}$$

The values of Δ at which the cavity is stable are located in two regions separated by the region of 'forbidden' values of Δ. The width of the latter increases with increasing the asymmetry parameter of the cavity $\gamma = (d_2 - f)/(d_1 - f)$.

Self-focusing, which appears with increasing pulse intensity in the medium, reduces the confocal parameter of the mode. This either improves the concentration of the lasing mode in the pumped region (soft aperture) or enhances the effective transmission through the aperture that is placed in a proper position in the cavity (hard aperture). This effective transmission, which is determined by the power P, can be found from the expression

$$\frac{\delta W}{W} = \frac{1}{W}\frac{\mathrm{d}W}{\mathrm{d}P}\bigg|_{P=0} P(t), \tag{7.14}$$

which gives the relation between the effective gain and power:

$$g = kP(t). \tag{7.15}$$

The dependence of k on Δ for different values of γ can be calculated. The almost symmetric configuration makes it possible to obtain the value of k that can be sufficient for the self-starting [92], but reduces the region of the stable operation. In practice, a compromise between the efficiency of self-amplitude modulation and the ability to withstand the external perturbations of the cavity is usually achieved at $1.5 < \gamma < 2$ by using a hard aperture placed near one of the end mirrors. The consideration of astigmatism shows that a slit should be used as an aperture. It was found that in the case of a soft aperture, the asymmetric configuration is preferable, and the better operation was achieved when in the second stability region, i.e., at the large distance between focusing mirrors [94].

8. Kerr-lens femtosecond laser

An important component of femtosecond lasers is a device for controlling and, if necessary, compensating GVD in the cavity. Of course, such a device should introduce minimal losses and should not distort the beam. In the simplest case, it consists of two prisms [37] (Fig. 11), of which the first one represent a dispersion element and the second one collects refracted beams into a parallel beam. To minimise the loss, the faces of the prism are oriented at Brewster's angle. The GVD can be represented, with a sufficient accuracy, in the form

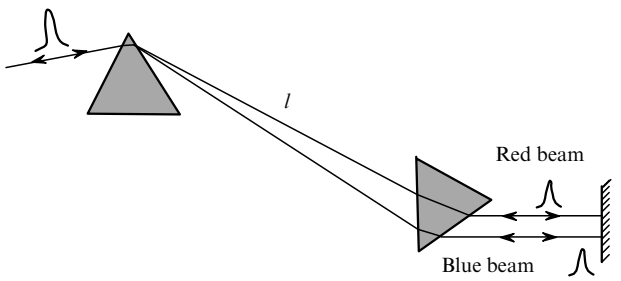

Figure 11. Prism GVD controller.

$$\frac{\mathrm{d}^2\Phi}{\mathrm{d}\omega^2} = (2\pi)^2/\omega^3\left(Ln'' - 4ln'^2\right), \tag{8.1}$$

where Φ is the phase; n' and n'' are the first- and second-order dispersions of the prism material; L is the active medium length; l is the distance between prisms. Although optical materials have positive dispersion in the visible and near-IR regions, GVD can continuously change (passing through zero) upon variation of L and (or) l. In practice, one of the prisms is moved along the bisectrix of the deviation angle, the value of l being fixed. For the laser operation, it is important to avoid the transverse displacement of the output spectral components. This is achieved in the Fabry–Perot configuration due to the reverse passage upon reflection of the beam from the mirror, while in the ring laser, an identical pair of prism is added. Of course, the value of GVD doubles in this case.

It is desirable to build a laser that has the minimum pulse duration and maximum pulse energy. These requirements are contradictory and, therefore, a compromise should be found. The pulse energy increases with the crystal length, whereas to shorten the pulse, one should decrease the crystal length in order to reduce the high-order dispersion.

The theory predicts that the minimum pulse duration can be achieved when the prism material is chosen so that the ratio of the third- and second-order dispersions would be minimal. For a Ti:sapphire laser, this material is fused silica. The pulse also shortens when the crystal length is reduced to 2–3 mm upon the appropriate increase in the Ti concentration to obtain the required gain. In this case, the high optical quality of the crystal should be retained. Note that as the crystal length is decreased, a serious problem of the heat removal appears despite the high heat conduction of sapphire. These problems have been solved, and laser pulses of 10 fs duration and lower have been obtained [96].

The limitations imposed by the high-order dispersion have been overcome due to the invention of the so-called chirped multilayer dielectric mirrors [97]. These mirrors, made of a proper material with the appropriate layer thickness, provide not only the maximum reflectivity in a broad spectral range (up to several hundreds of nanometres) but also a linear dependence of GVD on the wavelength over the entire spectrum. An ultrashort pulse reflected from such a mirror acquires the chirp of a certain magnitude and sign. The use of such mirrors allows one to exclude a prism GVD compensator. The schematic of a laser with such mirrors is shown in Fig. 12 [95]. The laser cavity consists of three chirped mirrors and an output mirror with the transmission of about 16 %. The region of maximum reflection lies between 690 and 900 nm. The cavity arm lengths are 118 and 68 cm and the radius of curvature of focusing mirrors $R = 50$ mm. The 5-W pump beam was focused by a lens ($f = 30$ mm) into a crystal. A hard aperture was placed near one of the chirped mirrors.

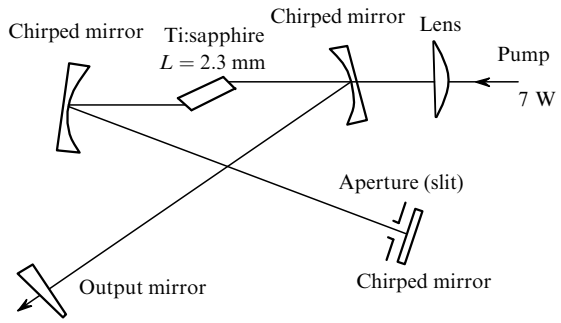

Figure 12. Schematic of a Ti:sapphire laser [95].

Under such conditions, 7.5-fs, 8-9-nJ ultrashort pulses were generated with a repetition rate of ~ 80 MHz. The peak power of these pulses exceeded 1 MW, which allowed the efficient conversion of the output radiation to the second

harmonic. By focusing radiation with a spherical mirror ($R = 25$ mm) into an LBO crystal of thickness 300 μm, the SHG efficiency was of about 20 %.

Note that the pulse energy inside the cavity greatly exceeds the output energy. By using the technique of fast extraction of radiation from the cavity (cavity damping) with the help of an acoustooptic switch, the output energy can substantially increased, however, at the expense of a decrease in the pulse repetition rate. In Ref. [98], 13-fs, 60 nJ ultrashort pulses were generated with a repetition rate of 200 kHz.

9. Amplification of ultrashort pulses

The energy of a single femtosecond pulse does not typically exceed 10 nJ and usually decreases with pulse shortening. Of course, the ultrashort-pulse energy can be increased up to several joules, however, this involves specific difficulties and, first of all, a huge gain of about $10^{10} - 10^{11}$. It is obvious that the pulse duration will increase due to the narrowing of the spectrum caused by such a gain. Another problem is the amplified spontaneous emission, which represents background light at the amplifier output, thereby limiting the achievable gain. In addition, a comparatively weak ultrashort pulse acquaires so high intensity during amplification that nonlinear effects appear (self-focusing, breackdown), which prevent the further amplification.

9.1 Multipass scheme

For the moderate gain of about 10^3, it is appropriate to use a multipass laser amplifier. An example of such an amplifier is shown in Fig. 13 [99]. The number of passages is limited by geometrical factors and the difficulties encountered upon focusing all beams in the active medium. In most cases, the typical number of passages is 4 – 8. The advantage of this scheme is the simplicity and the minimum number of optical elements (two mirrors and an amplifying element). Its principal drawback, except the complicated alignment, is that the amplified radiation is focused in the active medium. This results in rapid development of nonlinear restrictions. In principle, several such schemes can be used in a cascade, which, of course, will considerably complicate the system. Nevertheless, such systems are capable of generating ultrashort pulses with energy up to 50 μJ.

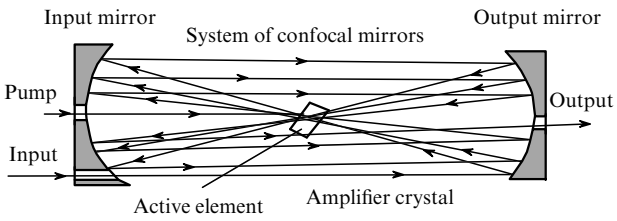

Figure 13. Schematic of a multipass amplifier [99].

Excimer amplifying systems represent a special case [71 – 76]. Ultrashort pulses generated in the visible range in these systems are amplified up to the power at which the efficient conversion to the second or third harmonic can be performed without a significant increase in the pulse duration. Then, the ultrashort pulse is amplified in wide-aperture excimer systems. The principal feature of this approach is a complete isolation of the amplifier components because preamplification and amplification in excimer modules occur at different wavelengths. This allows one to reduce substantially the level of amplified spontaneous emission. Terawatt powers were obtained for the first time using such excimer systems.

9.2 Chirped pulse amplification

To achieve the efficient gain, one should accumulate in the amplified pulse as much as possible of the energy stored in the active medium of the amplifier. For this purpose, it is desirable that the energy flux in the amplified beam would be of the order of the saturation energy flux for the active medium. Table 3 presents saturation energies for various amplifying media. One can see that, depending on the saturation energy, the media can be divided into two groups: dyes and excimers (the saturation energy is ~ 0.001 J cm^{-2}) and solids (the saturation energy is above 1 J cm^{-2}). The saturation energies required for obtaining the efficient energy output in solids correspond to ultrahigh intensities of femtosecond pulses, which substantially exceed the damage threshold of any solids.

Table 3. Saturation energies of active media used for amplification of ultrashort pulses.

Amplifying active medium	Saturation energy/J cm^{-2}	Spectral region/nm
Dyes	~0.001	Visible region
Excimers	~0.001	UV region
Ti : sapphire	~1	~800
Nd : glass	~5	~1054
Yb : glass	~40	~1000

This problem was successfully solved using a special technique of amplification of ultrashort pulses – the method of chirped pulse amplification [60]. The essence of the method is that a pulse being amplified passes through the delay line with large GVD, where it becomes chirped and its duration strongly increases (up to 10^4 times). Correspondingly, the peak power of the pulse decreases. Such a chirped pulse can be efficiently amplified to increase its energy thousands times. After amplification, the pulse again passes through the delay line, which has the same GVD but with the opposite sign. As a result, the chirp is compensated to zero and the pulse acquires the initial ultrashort duration. The key feature of this method is the use of optical systems that provide sufficiently large GVDs with opposite signs.

9.3 Diffraction-grating chirp controllers

As was shown, the magnitude of GVD and the chirp introduced by GVD can be controlled with a pair of prisms. However, a prism controller has a limited application because, provided its size is reasonable, it does not allow one to obtain CVD required for strong stretching and subsequent compressing ultrashort pulses. From this point of view, a GVD controller with a pair of reflection diffraction gratings is more efficient (Fig. 14), which, by the way, was proposed much earlier than the prism controller [36].

Diffraction gratings have a much greater angular dispersion than prisms, thereby providing much greater GVD (at a reasonable grating size). Although gratings exhibit 5–10 % losses and have a lower radiation resistance, these drawbacks can be eliminated in amplifier systems. The contemporary technology allows the gratings with linear

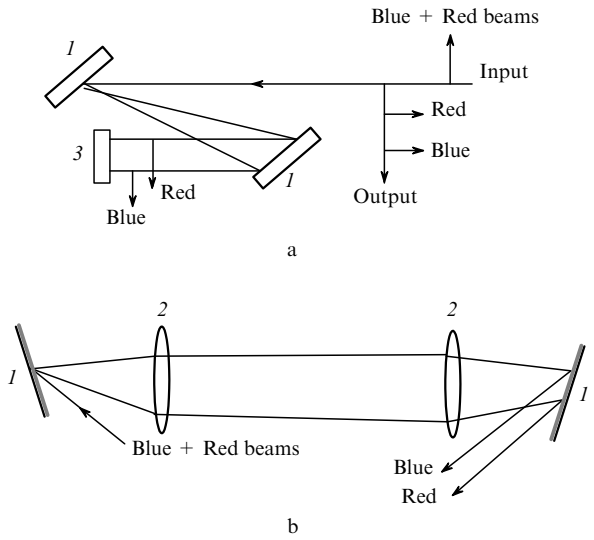

Figure 14. Schematic of a diffraction GVD controller for the pulse compression (a) and stretching (b): (*1*) diffraction gratings; (*2*) lenses; (*3*) retroreflector.

dimensions up to 1 m to be manufactured. Note that prism GVD controllers are mainly used in oscillators, while grating CVD controllers are used in amplifiers of ultrashort pulses.

The schematic of a controller with a pair of parallel gratings is shown in Fig. 14a. One can see that the optical path for long wavelengths is longer than that for short wavelengths. As a result, GVD emerges, which is defined as

$$\frac{d^2\Phi}{d\omega^2} = \left(-4\omega^2 cl/\pi d^2\right)\cos^3\beta, \qquad (9.1)$$

where l is the distance between the gratings; d is the grating period determined by the number of lines per millimetre; β is the dispersion angle. The GVD can be controlled by varying the distance between the gratings. Unlike a pair of prisms, a pair of gratings produces only negative GVD. To obtain positive GVD, a telescopic system is placed between the gratings (Fig. 14b) [100]. This system turns over the image so that the path for red beams becomes shorter than that for blue beams. Because the telescopic system should not introduce chromatic aberrations, a mirror system with the magnification -1 is used in practice. To simplify the construction of this system, plane mirrors are used, as a rule, which eliminate the displacement of the beams. A system of gratings with a telescope is used to stretch a femtosecond pulse, and a usual pair of gratings is employed for compressing the amplified chirped pulse.

The features of the method of amplifying chirped pulses in Nd : glass systems are considered in detail in review [101]. In such a system, the peak pulse power was obtained up to 30 TW [102].

9.4 The shortest high-power femtosecond pulses

The method of amplifying chirped pulses can be used not only for amplification, i.e., increasing the ultrashort pulse energy, but also for its shortening. If one does not stretch the pulse, by transforming it to the chirped pulse with the same spectral width, but forms the chirped pulse with a greater spectral width, then, by compressing the pulse, one can obtain a shorter pulse, whose duration corresponds to its spectral width. This approach was used in the first papers demonstrating this method [60]. The input chirped pulse was formed due to a combined action of SPM and GVD upon the propagation of a sufficiently intense pulse in a single-mode fibre. As a result, the pulse acquires an almost rectangular envelope with the duration that exceeds the initial one, but with a linear variation of the carrier frequency within its duration.

In Ref. [60], a Nd:YAG laser was used, which emitted 100-ps pulses. These pulses were coupled into a fibre of length 1.4 km, producing virtually rectangular output chirped pulses of duration 300 ps with a spectral width of 4 nm, which corresponds to the pulse duration equal to ~ 1 ps. After amplification up to the energy 7 mJ in a Nd : glass amplifier, the pulse passed through a pair of diffraction gratings. The loss in the compressor was about 50 %. As a result, 1.5-ps, 3 mJ pulses were generated.

The setup shown in Fig. 15 was uses for forming a chirped pulse with a broad spectral width and its compressing to a minimum duration [65]. The spectral broadening with chirping is achieved due to SPM upon the propagation of a high-power ultrashort pulse in a compressed inert gas (Ar, Kr). To provide a greater length of the nonlinear interaction and obtain the required broadening of the spectrum, the ultrashort pulse was coupled into in a hollow cylindrical capillary filled with inert gas at a pressure of several atmospheres.

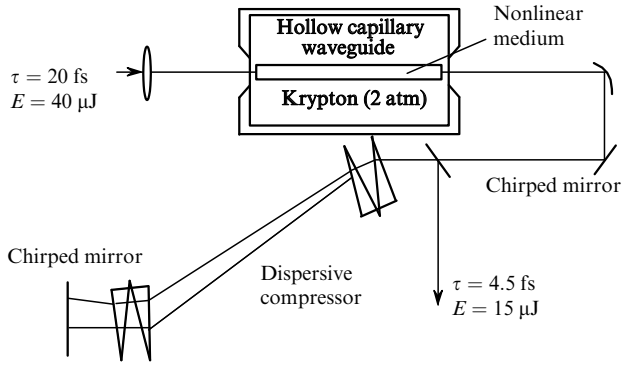

Figure 15. Schematic of the system for generation of 4.5-fs pulses [65].

This hollow waveguide represented a silica capillary of length 70 cm with an inner diameter of 140 μm. 20-fs, 40 μJ, 780-nm ultrashort pulses with a repetition rate of 1 kHz emitted by a system consisting of an oscillator and a Ti : sapphire amplifier were coupled into the fibre. The broadening of the spectrum achieved 130 THz. The pulse was compressed with a compressor consisting of prisms and chirped mirrors. The duration of pulses after compression was 4.5 fs and their energy was no less than 15 μJ.

10. Petawatt laser systems

The examples of a successful realisation of the principle of amplification of chirped pulses are ultrahigh-power laser systems built at the Lawrence Livermore National Laboratory (USA) and intended for studies in the field of inertial confinement fusion. The radiation peak power in these sys/tems achieves the petawatt level, which corresponds to the intensity of the focused beam of the order of 10^{21} W cm^{-2}.

10.1 Hybrid Ti : sapphire/Nd : glass laser

The setup studied in Ref. [61] used a femtosecond Ti:sapphire laser as a master oscillator. Because of a very broad gain bandwidth, this laser can emit at the emission wavelength of a Nd : glass laser (1054 nm). The laser pulse was stretched to 3 ns and amplified in a multistage system consisting of rods and discs pumped by flashlamps. The pulse repetition rate in this setup did not exceed a pulse per hour. The final amplification stage consisted of three disc moduli of the 'Nova' facility, which allow one to amplify laser beams 31.5 cm in diameter.

The energy at the amplifier output achieved 1120 J. The output beam was collimated to a diameter of 56.3 cm and was directed to a vacuum chamber containing a holographic grating compressor of one metre in size. The energy of the compressed pulse achieved 660 J and its duration could be varied from 430 fs to 20 ps. Thus, the maximum peak power exceeded 1 PW. The mirror focusing system provided the beam intensity up to 0.7×10^{21} W cm^{-2}.

10.2 Ti : sapphire laser

To achieve even greater pulse intensity, in the same laboratory the laser system was built that used Ti:sapphire both in an oscillator and an amplifier [62]. This laser produced ultrashort pulses of high quality.

In final amplifying stages of this setup, disc Ti : sapphire elements were used, which had an aperture of up to 10 cm and were pumped by the second harmonic of a 150-J 'Janus' Nd : glass laser. Focusing of radiation was performed with an off-axis paraboloid of diameter 15.24 cm and an aperture ratio of 1 : 2. The output beam divergence was only 1.5 times larger than the diffraction-limited divergence. The 75-fs output pulse energy achieved 15 J. Due to a high quality of the output beam and of focusing optics, the peak beam intensity exceeded 10^{21} W cm^{-2}.

10.3 Generation of relativistic-intensity femtosecond pulses with the kilohertz repetition rate

The development of laser systems producing high-power femtosecond pulses resulted in the possibility to study a new regime of the interaction of radiation with matter when the nonlinear nature of the interaction is caused by the relativistic motion of electrons in the light-wave fields. Such a regime emerges when the kinetic energy of an electron accumulated for one period of the electromagnetic field is comparable with the electron rest energy. In this case, the radiation intensity satisfies the relation

$$I\lambda^2 \geqslant 10^{18} \text{ W cm}^{-2} \text{ } \mu\text{m}^2.$$

Such a regime can be readily achieved in the above-described systems. However, they represent unique facilities and operate with a low repetition rate, which strongly prevents the performance of systematic studies. In the last years, compact (tabletop) and relatively inexpensive systems have been built [103, 104] capable of generating ultrashort pulses of duration 15 – 20 fs with an energy of 0.7 – 1 mJ, a pulse repetition rate of 1 kHz, and the unreproducibility of the output parameters of about 1 %. The high repetition rate, the high reproducibility and quality of the beam, close to the diffraction limit, are achieved due to pumping by high-power laser diodes. The high collimation of the laser beam is provided by the use of a computer-controlled adaptive mirror in the optical amplification system of chirped pulses. The high-power laser radiation can be focused with help of high-quality optics (an off-axis paraboloid with the aperture ratio of 1 : 1) into a small spot of about 1 μm, resulting in the ultrahigh intensity at the relativistic level.

Note that these laser systems represent unique sources of the concentrated optical radiation. Indeed, the energy 1 mJ corresponds approximately to 10^{16} photons, the area of the focal spot is $\sim 10^{-8}$ cm^2, and the pulse spatial extension is 6×10^{-4} cm. This means that the concentration of photons in the focal region achieves 10^{27} photon cm^{-3}, which exceeds by several orders of magnitude the density of atoms in solids.

11. Applications of ultrashort-pulse lasers

The unique properties of femtosecond lasers have found wide applications in varies fields of science, technology, and medicine. The efficiency of applications of ultrashort pulses can stem from their extremely short duration and associated low time coherence, enormous peak power and intensity, large time coherence and average power of a train of ultrashort pulses. Below, basic applications of ultrashort pulses and their relevant key parameters are listed. Because it is impossible even briefly consider all possible applications of ultrashort pulses within the scope of a single review, we mention here only the applications related to the ultimate parameters of these pulses, which have been recently implemented.

Applications in science

1. Applications based on the extremely short pulse duration:
   – nonlinear optics;
   – fibre optics and optical solitons;
   – studies of ultrafast phenomena by the pump-probe method and time-resolved spectroscopy;
   – two- and three-photon microscopy;
   – femtochemistry;
   – terahertz beams and coherent time Fourier spectroscopy.
2. Applications based on the high coherence of a continuous train of ultrashort pulses:
   – precision spectroscopy, including multiphoton transitions;
   – absolute measurements of optical frequencies and optical frequency standards.
3. Applications based on the high power, intensity, and strength of the light-wave fields:
   – laser plasma and X-ray sources;
   – relativistic regime of the interaction of radiation with matter;
   – acceleration of electrons;
   – collimated X-ray and γ-ray beams;

– experiments on nonlinear quantum electrodynamics;
– initiation of photonuclear reactions and fast ignition in inertial confinement fusion.

4. Applications related to the high power of pulses of duration of several optical cycles;
– generation of high harmonics up to X-rays;
– generation of VUV and soft X-ray pulses of the attosecond duration.

Applications in technology

1. Ultrafast optoelectronics and oscilloscopes with the subpicosecond resolution.
2. Control of elements for microelectronics.
3. Fibre-optic communication with the bit rate of ~ 1 Tbit c^{-1}.
4. Precision machining.
5. Terahertz imaging systems.
6. Isotope separation.

Applications in medicine

1. Optical coherent tomography.
2. Precision surgery.
3. Fabrication of micro-stents in cardiology.
4. Two-photon photodynamic therapy.

11.1 Optical coherent tomography

This application is based on the use of radiation with extremely low time coherence, which in inherent in ultrashort pulses. Ultrashort-pulse optical tomography allows imaging in strongly scattering media. Its principle is similar to ultrasonic introscopy, which is widely used in medicine (ultrasonic diagnostics). The spatial resolution of this method can be substantially improved due to the use of optical radiation. Although strong scattering of light in biotissues prevents imaging at a depth exceeding 2–3 mm, nevertheless this technique proved to be useful for microsurgery.

The method is based on he interference between a laser beam scattered by an object and a reference beam. By varying the delay between these beams, one can study the interference with a signal coming from different depths. The delay is scanned continuously, resulting in the frequency shift of one of the beams due to the Doppler effect. This allows one to separate the interference signal against an intense background caused by scattering. By scanning and processing signals, various layers of the tissue under study are imaged (tomography). Modern computers provide fast signal processing and allow real-time imaging. The spatial resolution in depth is determined by the time coherence of a light source. The lower the coherence, the lower minimal thickness of the image section of the object under study.

Usually, a superluminescence diode is employed as a radiation source. The width of its spectrum (32 nm) provides the spatial resolution equal to 11 μm. The efficiency of this method has been demonstrated in Ref. [105]. In Ref. [80], a Ti:sapphire laser emitting pulses shorter than 5 fs has been used as a radiation source. This improved the spatial resolution to 1.5 μm and provided an increase in the sensitivity by increasing the incident power. As a result, images of cells of biotissues were obtained with the spatial resolution close to the diffraction limit of optical microscopy, but from the depth of tissues strongly scattering light.

Thus, the authors of Ref. [80] have demonstrated the imaging of cells *in vivo*, including their nuclei, which allows one, for example, to perform biopsy of oncology tissues directly during the operation. This technique can be also used in the medical treatment of glaucoma.

11.2 Optical frequency standards

This application is related to the high time coherence of a continuous train of femtosecond pulses. To create optical frequency standards, the optical frequency (a few hundreds of terahertz) should be measured relative to the International Second Standard, which is measured from the hyperfine splitting of the ground level of a cesium atom (in the region of 9.2 GHz).

In the near past this has been performed using the consecutive frequency multiplication to obtain the optical frequency subject to measuring. Because of the necessity of covering a broad frequency range, these multiplication chains represented huge constructions containing the intermediate stabilised far- and mid-IR lasers, nonlinear elements, measuring instruments, etc. These facilities require a very careful maintenance and each of them generates only a certain optical frequency.

Such a multiplication chain can be replaced by a comb-oscillator generating optical frequencies separated by the frequency interval lying in the radio frequency range. These frequencies overlap the interval between the laser frequency f_{opt} being measured and its second harmonic $2f_{opt}$ (Fig. 16). If the comb interval is stable and is measured sufficiently accurately, then, having measured the difference Δf_1 between f_{opt} and the nearest frequency of the red part of the comb, as well as the difference Δf_2 between $2f_{opt}$ and the nearest frequency of the blue part of the comb, one can count the number N of frequencies between them and thereby determine the required frequency. One can see from Fig. 16 that the optical frequency f_{opt} is related to the frequencies measured in the radio frequency range by a simple expression $\Delta f_1 + N\Delta F + \Delta f_2 = 2f_{opt} - f_{opt} = f_{opt}$.

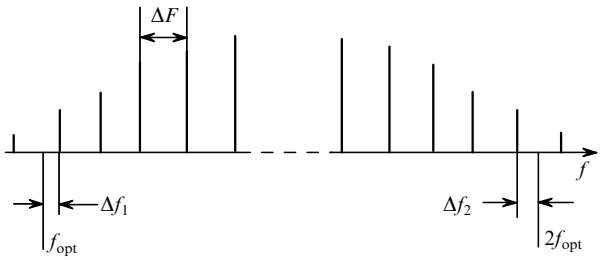

Figure 16. Schematic of measurements of the absolute frequency with the help of a comb-oscillator.

Because the spectral width of radiation from the comb-oscillator is inversely proportional to the pulse duration, which can be shorter than 5 fs, it is possible to create the frequency comb extending by several tens of terahertz. It was shown in Ref. [81] that the pulse repetition rate, which can be easily measured and controlled, is equal to the intermode interval within an accuracy of measurements (about 10^{-16}) and that the frequency comb is uniform with an accuracy of $\sim 10^{-16}$ even in the case of the spectral broadening in a silica microstructure fibre (the so-called photonic crystal fibers [84]). This method has been used for the precision measurement of the $1S-2S$ transition frequency in the hydrogen atom [106], which proved to equal to 2 466 061 413 187 103(46) Hz. Recently, by using 70–100 fs ultrashort pulses from a Ti : sapphire laser, the frequency comb was obtained in a cone-tapered fibre that covered the spectral range from 370 to 1545 nm [107].

It should be noted that the idea of using a continuous train of ultrashort pulses for precision measurements of optical frequencies has been first proposed by V P Chebotaev [108]. His proposal was in essence an original extension of the method of separated oscillating fields in the radio frequency range, for the development of which N Ramsey has been awarded with the Noble Prize, to the optical region.

11.3 Precision material machining

Material machining by ultrashort laser pulses is an important technological application of lasers, which requires high-average-power lasers. The laser material machining is based on the local thermal action and subsequent ablation – the removal of the material caused by its melting, evaporation, and shearing. The laser micromachining is employed in the technology of modern electronics. Because the minimal size of the focal spot decreases with the laser wavelength, UV excimer lasers are successfully used for micromachining. However, their radiation is strongly absorbed by many transparent materials so that only the surface of these materials can be processed. For lasers with $\lambda < 200$ nm (an ArF laser emitting at 193 nm), the problem of radiation damage of the focusing optics also exists. Ultrashort pulses can be used both for the surface and bulk machining (of transparent materials) with an accuracy that is not worse than that achieved with excimer lasers, but, in contrast to the latter, in the visible range [109].

Ultrashort-pulse lasers are characterised by high radiation intensity, which increases the role of multiphoton processes. This circumstance and exclusively short duration of the interaction fundamentally changes the mechanism of interaction of the radiation with matter. Because of the high intensity of ultrashort pulses, seed electrons are produced due to multiphoton ionisation rather than by impurities. For this reason, there is no statistic scatter in the breakdown threshold at the sufficiently high pulse intensity and, therefore, the breakdown and the energy deposited to the medium can be controlled. Due to the high strength of the electromagnetic field, electrons are heated to high temperatures and then, after the pulse termination, the energy transfer occurs from electrons to ions. Because the initial electron temperature is very high, the ion temperature also can become greater than in the case of long pulses. A greater part of the substance will be evaporated inside the focal volume, by rapidly passing through the melting phase. Because the liquid phase contains a smaller amount of the substance during the ablation, the melt drops disappear and the boundary being processed becomes sharp.

In experiments [109], holes 0.3 μm in diameter were produced in a silver film and less than 1 μm in fused silica, although in the first case the 200-fs, 790-nm pulses from a Ti : sapphire laser were focused into a spot of diameter 3 μm, and in the second case, 60-fs pulses were focused into a spot of diameter 5 μm. Such small hole sizes (less than the diffraction-limited one) were achieved due to an accurate control of the ultrashort-pulse intensity and obtaining the ablation threshold within a small area at the centre of the focal spot.

These applications require the use ultrashort-pulse lasers with a high average power. In particular, a diode-pumped Yb : YAG laser can be employed [110]. The problem of heat removal, which is crucial in the case of high average power, was solved in this laser by using an active element in the form of a disc with a highly reflecting coating of thickness 220 μm, which was placed on a cooling finger. The laser emitted 730-fs, 1030-nm pulses with an average power of 16.2 W.

11.4 Ultrahigh-intensity applications

Due to the high concentration of radiation energy in ultrashort pulses, they have the ultrahigh intensity and produce superstrong electromagnetic fields. This results in the emergence of new regimes of the interaction of laser radiation with matter, in particular, with plasma. These regimes are caused by the unique parameters of modern ultrashort-pulse lasers.

First of all this is the short pulse duration (less than 100 fs), which is shorter than any time intervals determining hydrodynamic motions in a plasma. The enormous strengths of electric and magnetic fields produced by ultrashort pulses also play an important role. At intensities of 10^{21} W cm^{-2}, which can be produced at present, the electric-field strength achieves 10^{12} V cm^{-1}, which is more than 100 times greater than the strength of the Coulomb field on the first Bohr orbit of the hydrogen atom. Finally, the enormous energy density, which amounts to 3×10^{10} J cm^{-3}, corresponds to the black body temperature of about 10 keV. Such magnitudes are typical for a nuclear explosion. Under such conditions, the motion of an electron becomes purely relativistic. Because of the simultaneous action of the Lorentz force, the electron in a linearly polarised wave traces a trajectory in the form of a figure eight and its motion becomes strongly nonlinear. Consider some applications of ultrahigh-power ultrashort pulses.

Generation of high harmonics. The interaction of intense laser radiation with atoms of inert gases results in the generation of high harmonics of the fundamental frequency [111], their frequencies extending to the VUV and soft X-ray regions. The relevant processes are discussed in detail in review [112].

When the laser radiation intensity exceeds 10^{14} W cm^{-2}, the photoionisation of atoms becomes important, which can be treated as quasi-static tunneling in a strong electric field of the light wave superimposed on the Coulomb field of the atomic nucleus. The emitted electrons are accelerated in the field of the laser wave and then can experience collisions either with an ion from which they were removed or with other neighbouring ions. Upon recombination, photons are emitted with the energy that is equal to a sum of the ionisation potential and the kinetic energy acquired in the laser-wave field. The high harmonics are generated because this elementary process repeats quasi-periodically at the laser radiation frequency.

If the pulse duration is shortened to a few optical cycles, the ionisation can occur for a fraction of the optical cycle. In this case, an electron has no time to be removed from an atom. In other words, such short pulses allow one to abruptly 'switch on' ultrahigh-intensity fields, which exceed the intraatomic field that holds the electron in the atom, and thereby subject the nonlinear object (atom + electron) to the action of fields that greatly exceed the ionisation threshold. In this case, the nonlinear interaction becomes substantially dependent on the phase of the electromagnetic wave. This is illustrated by the evolution of the high-harmonic intensity (in VUV and X-ray regions) for two different values of the absolute phase in the wavelength band equal to 10 % of $\lambda = 3.2$ nm [113] (Fig. 17). The

calculation was performed for the interaction of linearly polarised 5-fs, 2×10^{15} W cm^{-2} laser pulses at $\lambda = 750$ nm with helium at a pressure of 500 Torr. One can see that for the same envelope the intensity of short-wavelength pulse and its shape strongly depend on the phase. This demonstrates the first possibility of studying nonlinear optical effects, which directly depend on the absolute phase of the light wave [85].

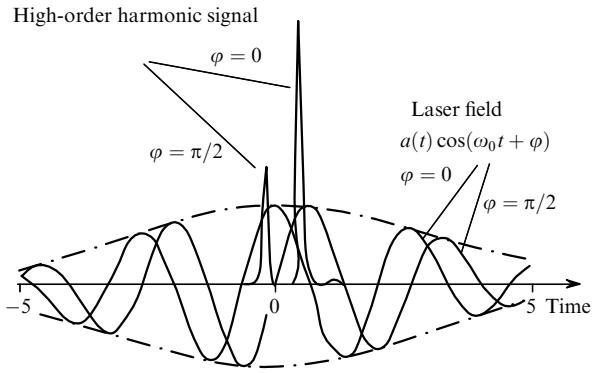

Figure 17. Evolution of the high-order harmonic intensity (VUV, soft X-rays) calculated for two different values of the absolute phase [113].

The high-harmonic photons with maximum energies are produced by electrons with the maximum energy, which they acquire in a narrow interval of variation of the light-wave phase. This means that short-wavelength radiation in the VUV and soft X-ray regions will be concentrated within the interval that represents a small fraction of the optical cycle (Fig. 17). Therefore, the possibility appears to generate pulses with the attosecond duration. This possibility was experimentally confirmed in Ref. [114].

The efficiency of high-harmonic generation can be increased by using the phase matching between the fundamental frequency and high harmonics. In this case, a capillary tube serves as a cell with inert gas. The phase matching results in the increase in the generation efficiency by two-three orders of magnitude. In experiments [115], a Ti:sapphire laser was used, which emitted 26-fs, 20 mJ pulses with a repetition rate of 1 kHz at a wavelength close to 800 nm. When the capillary was filled with helium, high harmonics were observed up to 299 order at a wavelength of ~ 2.7 nm (460 eV). Thus, a source of collimated coherent soft X-rays was in fact created. The importance of building such a source is explained by the fact that its radiation falls into the so-called 'water window' (2.3 – 4.4 nm). The emission in this region corresponds to the edges of the K-bands of oxygen and carbon and is absorbed by water weaker than by carbon. This allows highly contrast imaging of biological microobjects containing carbon in water, i.e., *in vivo*. So far, synchrotron radiation from very large electron accelerators has been used for this purpose.

Nonlinear quantum electrodynamics. At enormous intensities of the order of 10^{30} W cm^{-2}, vacuum already becomes a nonlinear medium and electron-positron pairs are created in such a superstrong light field. The electric-field strength E required for the creation of such a pair is $2m^2c^3/eh = 1.3 \times 10^{16}$ V cm^{-1}.

One can see that the possibilities of contemporary lasers are still very far from generating such enormous fields. However, the experimental situation with a critical field can be implemented by using superrelativistic electrons. A moving electron entering the field of an electromagnetic wave 'see' it at a frequency changed by a factor of η, where η is the relativistic factor. The effective laser field also increases by a factor of η. To achieve the critical field with the help of contemporary lasers, the relativistic factor η should be $\sim 10^5$, i.e., the electron energy should be equal to 50 GeV. Such energies can be obtained in modern accelerators.

Two effects of nonlinear quantum electrodynamics can be observed: nonlinear Compton scattering, when more than one photon are scattered by an electron ($e^- + nhv_L \rightarrow e^- + hv_\gamma$, where v_L and v_γ are frequencies of the laser and gamma quanta, respectively), and the creation of electron-positron pairs. The interaction of photons with a relativistic electron produces gamma rays. The interaction of the high-energy gamma quantum with a superstrong laser field can result in the multiphoton creation of an electron-positron pair: $hv_\gamma + nhv_L = e^- + e^+$.

Both these effects have been observed experimentally [116, 117]. The experiments were performed at the Stanford Linear Accelerator Center. The accelerator has the following parameters: the electron energy was 46.6 GeV, the electron pulse (bunch) duration was 7 ps, and the repetition rate was 10 – 30 Hz. The second harmonic from a Nd : glass laser was used. The parameters of the laser setup were as follows: the pulse energy at the fundamental frequency was 2 J and that at the second harmonic frequency was 0.4 J, the pulse duration was 1.5 ps, and the repetition rate was 0.5 Hz. The main difficulty of the experiment was overlapping the focused laser pulse and the electron bunch in space and time (within tens of micrometers and fractions of picoseconds, respectively). The authors of [116, 117] have observed for the first time the nonlinear Compton scattering involving up to four laser photons, as well as the creation of electron-positron pairs in collisions of gamma quanta with laser photons. This was the first experimental demonstration of inelastic scattering of light by light involving real photons.

Photoinduced nuclear reactions. At intensities of 10^{19} – 10^{20} W cm^{-2}, electrons experience relativistic oscillations in the light-wave field at which their kinetic energy increases to several megaelectronvolts. The interaction of such ultrahigh-intensity radiation with solid targets produces a relativistic plasma, in which the electrons can acquire even greater energy. The mechanisms of such acceleration of electrons were theoretically studied in Ref. [118]. The use of relativistic electrons in optically induced nuclear reactions was proposed in Ref. [119].

The relativistic interaction of light with matter was experimentally studied using ultrahigh-power laser facilities. The laser beam power used in Ref. [120] achieved 50 TW. By focusing such a beam onto various solid targets, electrons with energies of tens of megaelectronvolts were produced, which, in turn, created gamma-quantum beams that stimulated photonuclear (γ, n) reactions. In these reactions, isotopes ^{11}C, ^{38}K, ^{62,64}Cu, ^{63}Zn, ^{106}Ag, ^{140}Pr, and ^{180}Ta were produced, which were detected by the methods of nuclear physics. In addition, the fission of ^{238}U was observed in these experiments.

In Ref. [121], a petawatt laser facility was used which irradiated targets by focused beams with a pulse duration of

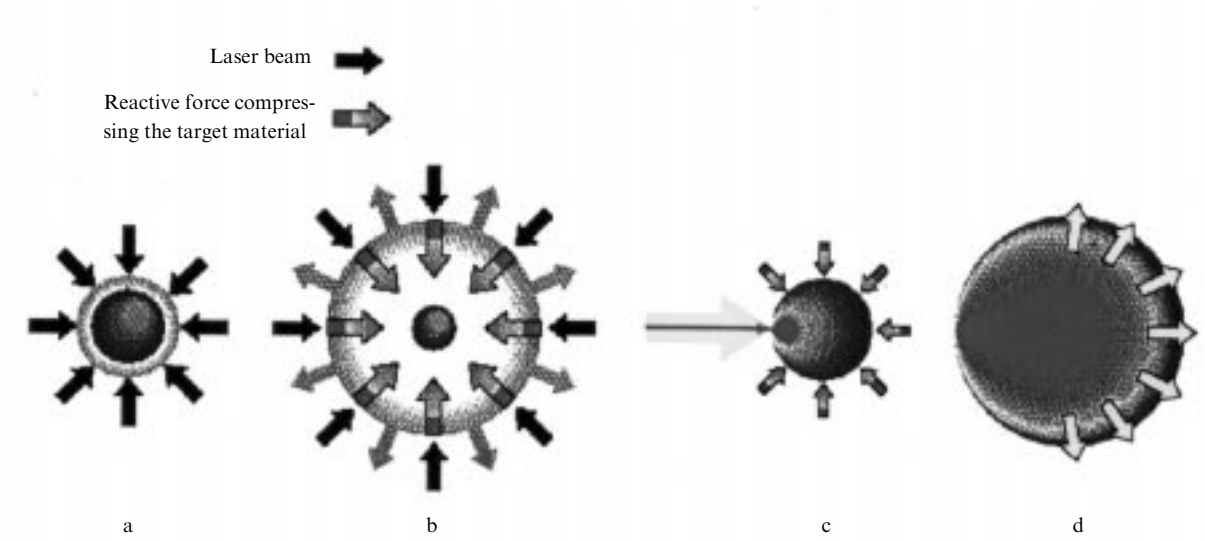

Figure 18. Schematic of fast ignition in inertial confinement fusion showing the four main steps: symmetric irradiation of a spherical target (a), target compression (b), channel formation in a plasma surrounding the target (c), and the plasma heating by hot electrons and ignition of the entire target (d) [124].

450 fs and an energy of 260 J. The focused beam intensity exceeded 10^{20} W cm^{-2}, resulting in the electron energy acquired in the light-wave field equal to 3 MeV. The electron energy in a plasma produced on the target achieved 100 MeV. In this paper, (the γ, n) reactions and fission of ^{238}U were also observed.

Fast ignition of inertial confinement fusion. With the advent of ultrahigh-power laser facilities based on amplification of chirped pulses, a new concept of fast ignition of inertial confinement fusion was proposed [122]. The essence of this concept is that at laser intensities of 10^{21} W cm^{-2} and greater, electrons acquire the energy of about 1 MeV in the laser-wave field. Hot electrons rapidly equilibrate in the dense plasma by heating ions up to 5–20 keV. However, to produce the efficient heating of ions, the path length of hot electrons in plasma should be comparable with the diameter of a focused laser beam.

Because the initial plasma density is insufficient for this purpose, even if it is equal to the density of a solid, it is proposed to compress a spherical target by irradiating it symmetrically by high-power beams (Fig 18a). Such symmetrical irradiation is used in laser facilities used in inertial confinement fusion studies. Upon rapid heating of the target surface, the expanding plasma produces the reactive force, which compress the target material (Fig. 18b). It has been demonstrated [123] that the uniform irradiation of a spherical target by nanosecond laser pulses of energy 9 kJ resulted in the target compression up to a density of 600 g cm^{-3}. However, the dense plasma in the target core is surrounded by a plasma layer, the so-called plasma corona, whose density gradually decreases to zero. To heat the plasma by a high-power ultrashort pulse, the pulse should be delivered to the surface of the dense core. For this purpose, the density profile of plasma is modified with the help of an additional laser pulse (Fig. 18c). The target is irradiated by a 50-ps pulse with a profiled intensity, which provides the excess of the light pressure over the gas-kinetic pressure in plasma. As a result, a narrow channel is produced in the plasma corona, through which the main ultrahigh-power ($E = 1 - 10$ kJ) ultrashort pulse ($\tau \simeq 1$ ps) is directed. This beam produces hot electrons that ignite the target material (Fig. 18d). The calculations showed that this concept of inertial confinement fusion will require a reduced laser drive energy compared to the traditional approach based on the use of nanosecond laser pulses.

12. Conclusions

At present, ultrashort-pulse lasers have gained a great development. The methods for generating laser pulses of duration not exceeding 5 fs have been suggested and demonstrated. The peak power of femtosecond pulses exceeds 10^{15} W and the intensity of the focused beam achieves 10^{21} W cm^{-2}.

The efficient and compact lasers systems capable of generating ultrashort, ultrahigh-power pulses open up excellent prospects for applications in science, technology, and medicine. The possibility of studies of nonlinear optics in the relativistic regime has appeared. New methods for generating X-rays and gamma rays and acceleration of electrons have been developed. Technological applications include microelectronics, the development of fibre-optic communication with a bit rate of ~ 1 Tbit s^{-1}, new methods for micromachining, and creation of optical memory devices. In medicine, new methods of microscopy, optical tomography, and sophisticated surgery operations have been demonstrated.

It is also very important that contemporary laser systems facilitate the transfer of some trends in 'big science' to university laboratories. Note that the intensities of the order of 10^{21} W cm^{-2} correspond to gigabar pressures and gigagauss magnetic fields. This opens up the outlook for studies that can be called the laboratory astrophysics.

References

1. *Ultrashort Laser Pulses,* Shapiro S, ed. (New York: Wiley, 1978; Moscow: Mir, 1981)
2. Herrmann J, Wilhelmi B *Lasers for Ultrashort Light Pulses* (Amsterdam: North-Holland, 1987; Moscow: Mir, 1986)

3. Diels J-C, Rudolph W *Ultrashort Laser Pulse Phenomena: Fundamentals, Techniques, and Applications on Femtosecond Time Scale* (Boston: Academic Press, 1996)
4. *Femtosecond Laser Pulses*, Rulliere C, ed. (Berlin: Springer-Verlag, 1998)
5. Hargrove L E, Fork R I, Pollack V A *Appl. Phys. Lett.* **5** 4 (1964)
6. Mocker H W, Collins R J *Appl. Phys. Lett.* **7** 270 (1965)
7. DeMaria A J, Stetser D A, Heynau H *Appl. Phys. Lett.* **8** 174 (1966)
8. Weber H P *J. Appl. Phys.* **38** 2231 (1967)
9. Armstrong J A *Appl. Phys. Lett.* **10** 16 (1967)
10. Giordmaine J A, Rentzepis P M, Shapiro S I, Wecht K W *Appl. Phys. Lett.* **11** 218 (1967)
11. DeMaria A J, Glenn Jr. W H, Brienza M J, Mack M E *Proc. IEEE* **57** 2 (1969)
12. Zavoiskii E K, Fanchenko S D *Dokl. Akad. Nauk SSSR* **108** 216 (1956)
13. Malyutin A A, Shchelev M Ya *Pis'ma Zh. Eksp. Teor. Fiz.* **9** 445 (1969)
14. Korobkin V V, Malyutin A A, Shchelev M Ya *Pis'ma Zh. Eksp. Teor. Fiz.* **11** 188 (1970)
15. Shchelev M Ya, Richardson M C, Alcock A J *Appl. Phys. Lett.* **18** 354 (1971)
16. Kryukov P G, Letokhov V S *Usp. Fiz. Nauk* **99** 169 (1969)
17. Basov N G, Kryukov P G, Letokhov V S, Matveets Yu A *Zh. Eksp. Teor. Fiz.* **56** 1546 (1969)
18. Basov N G, Drozhbin Yu A, Kryukov P G, Lebedev V B, Letokhov V S, Matveets Yu A *Pis'ma Zh. Eksp. Teor. Fiz.* **9** 428 (1969)
19. Letokhov V S Zh. Eksp. Teor. Fiz. **55** 1077 (1968)
20. Kryukov P G, Letokhov V S IEEE J. Quantum Electron. **8** 766 (1972)
21. Zakharov S D, Kryukov P G, Matveets Yu A, Chekalin S V, Churilova S A, Shatberashvili O B, in: *Kvantovaya Elektronika 5*(17) 52 (1973)
22. Zherikhin AN, Kovalenko V A, Matveets Yu A, Chekalin S V *Kvantovaya Elektron.* **2**/1 377 (1974/5) [*Quantum Electron.* **4**(2) 377 (1974)]
23. Von der Linde D, Berneker O, Kaizer W *Opt. Commun.* **2** 149 (1970)
24. Von der Linde D *IEEE J. Quantum Electron.* **8** 328 (1972)
25. Zherikhin A N, Kryukov P G, Matveets Yu A, Chekalin S V *Kvantovaya Elektron.* **1** 956 (1974) [*Quantum Electron.* **4** 525 (1974)]
26. Schmidt W, Schafer F P *Phys. Lett. A* **2**6 558 (1968)
27. Kogelnik H W, Ippen E P, Dienes A, Shank C V *IEEE J. Quantum Electron.* **8** 373 (1972)
28. Ippen E P, Shank C V, Dienes A *Appl. Phys. Lett.* **21** 348 (1972)
29. Ippen E P, Shank C V *Appl. Phys. Lett.* **27** 488 (1975)
30. Bradley D J, Liddy B, Roddie A G, Sibbett W, Sleat W E *Opt. Commun.* **3** 426 (1971)
31. Arthurs E G, Bradley D J, Roddie A G *Appl. Phys. Lett.* **23** 88 (1973)
32. Arthurs E G, Bradley D J, Roddie A G *Opt. Commun.* **8** 118 (1973)
33. New G H C *IEEE J. Quantum Electron.* **10** 115 (1974)
34. Fork R L, Greene B I, Shank S V *Appl. Phys. Lett.* **38** 671 (1981)
35. Dietel W, Fontaine J, Diels J-C *Opt. Lett.* **8** 4 (1983)
36. Treacy E B *Phys. Lett. A* **28** 34 (1968)
37. Fork R L, Martinez O E, Jordan J P *Opt. Lett.* **9** 150 (1984)
38. Valdmanis J A, Fork R L, Jordan J P *Opt. Lett.* **10** 131 (1985)
39. Moulton P F *J. Opt. Soc. Am. B* **3** 125 (1986)
40. Payne S A, Chase L L, Smith L R, Kway W L, Newkirk H W *J. Appl. Phys.* **66** 1051 (1999)
41. Smith L K, Payne S A, Kway W L, Chase L L, Chai B H T *IEEE J. Quantum Electron.* **28** 2612 (1992)
42. Petricevic V, Gayen S K, Alfano R R *Opt. Lett.* **14** 612 (1989)
43. Angert N B, Borodin N I, Garmash V M, Zhitnik V A, Okhrimenchuk A G, Syuchenko O G, Shestakov A V *Kvantovaya Elektron.* **15** 113 (1988) [*Quantum Electron.* **18** 73 (1988)]
44. Heinz P, Lauberau A *J. Opt. Soc. Am. B* **6** 1574 (1979)
45. Agnesi A, DelCorno A, DiTrapani P, Fogliani M, Reali G C, Diels J-C, Yeh C-Y, Zhao X M, Kubecek V *IEEE J. Quantum Electron.* **28** 710 (1992)
46. Dalstrom L *Opt. Commun.* **5** 157 (1972)
47. Mollenauer F, Stolen R H *Opt. Lett.* **9** 13 (1984)
48. Blow K J, Wood D *J. Opt. Soc. Am. B* **5** 629 (1988)
49. Mark J , Liu L Y, Hall K L, Haus H A, Ippen E P *Opt. Lett.* **14** 48 (1989)
50. Kean P N, Zhu X, Crust D W, Grant R S, Langford N, Sibbett W *Opt. Lett.* **14** 39 (1989)
51. Haus H A, Fujimoto J G, Ippen E P *IEEE J.Quantum Electron.* **28** 2086 (1992)
52. Keller U *Appl. Phys. B* **58** 347 (1994)
53. Spence D E, Kean P N, Sibbett W *Opt. Lett.* **16** 42 (1991)
54. Morgner U, Kartner F X, Cho S H, Chen Y, Haus H A, Fujimoto J G, Ippen E P, Schneuer V, Angelov G, Tshudi T *Opt. Lett.* **24** 411 (1999)
55. Ober M H, Haberl F, Fermann M E *Appl. Phys. Lett.* **60** 2177 (1992)
56. Fermann M E, Galvanauskas A, Harter D, Windeler R S *Opt. Lett.* **23** 1840 (1998)
57. Agrawal G P *Nonlinear fiber optics* (New-York, Academic Press, 1989)
58. Fermann M E, Galvanauskas A, Sucha G, Harter D *Appl. Phys. B* **65** 259 (1997)
59. Nelson L E, Jones D J, Tamura K, Haus H A, Ippen E P *Appl. Phys. B* **65** 275 (1997)
60. Strikland D., Mourou G. *Optics Comms*, **56**, 219 (1985)
61. Perry M D, Pennington D, Stuart B C, Tietbohl G, Britten J A, Brown C, Herman S., Golik B, Kartz M, Miller J, Powell H T, Vergino M, Yanovsky V *Opt. Lett.* **24** 160 (1994)
62. Bonlie J, Patterson F, Price D, White B, Springer P *Appl. Phys. B* **70** 155 (2000)
63. Fork R L, Brito Cruz C H, Becker P C, Shank C V *Opt. Lett.* **12** 483 (1987)
64. Nisoli M, DeSilvestri S, Svelto O *Appl. Phys. Lett.* **68** 2793 (1996)
65. Sartania S, Cheng Z, Lenzner M, Tempea G, Spielmann Ch, Krausz F, Ferencz K *Opt. Lett.* **22** 1562 (1997)
66. Dianov E M, Belov A B, Bufetov I A, Protopopov V N, Gur'yanov A N, Gusovskii D D, Kobis' S V *Kvantovaya Elektron.* **24** 3 (1997)

67. Kurkov A S, Karpov V I, Laptev A Yu, Medvedkov O I, Dianov E M, Gur'yanov A N, Vasil'ev S A, Paramonov V M, Protopopov V N, Umnikov A A, Bechkanov N I, Artyushenko V G, Fram Yu *Kvantovaya Elektron.* **27** 239 (1999)
68. Szatmari S, Schaefer F P, Mueller-Horsche E, Mueckenheim W *Opt. Commun.* **63** 5 (1987)
69. Glownia J H, Misewich J, Sorokin P P *J. Opt. Soc. Am. B* **4** 1061 (1987)
70. Endoh A, Watanabe W, Sarukura S, Watanabe S *Opt. Lett.* **14** 353 (1989)
71. Rolland C, Corcum P B *Opt. Commun* **59** 64 (1986)
72. Reid D T, Padgett M, McGowan C, Sleat W E, Sibbett W *Opt. Lett.* **22** 233 (1997)
73. Delong K W, Trebino R, Hunter J, White W E *J. Opt. Soc. Am. B* **11** 2206 (1994)
74. Chilla J, Martinez O *IEEE J. Quantum Electron.* **27** 1228 (1989)
75. Baltuska A, Pschenichnikov M S, Wiersma D A *Opt. & Phot. News* **9**(12) 53 (1998)
76. Mazurenko Yu T Kvantovaya Elektron. **12** 1235 (1985)
77. Zubov V.A., Kuznetsova T.I. *Laser Phys.*, **2**, 73 (1992).
78. Iaconis C, Walmsley I A *Opt. Lett.* **23** 792 (1998)
79. Dorrer C, DeBeauvoir B, LeBlank C, Ranc S, Rousseau J-P, Rousseau P, Chambaret J-P, Salin F *Opt. Lett.* **24** 1644 (1999)
80. Drexler W, Morgner U, Kärtner F X, Pitris C, Boppart S A, Li X D, Ippen E P, Fujimoto J C *Opt. Lett.* **24** 1221 (1999)
81. Reichert J, Niering M, Holzwarth R, Weitz M, Udem Th, Hänsch T W *Phys. Rev. Lett.* **84** 3232 (2000)
82. Marioka T, Kawanishi S, Mori K, Saruwatari M *Electron. Lett.* **30** 1166 (1994)
83. Collings B S, Mitchell M L, Boivin L, Knox W H *IEEE Photon. Technol. Lett.* **12** 906 (2000)
84. Diddams S A, Jones D J, Jun Ye, Cundiff S T, Hall J L, Ranka J K, Windeler R S, Holzwarth R, Udem Th, Hänsch T W *Phys. Rev. Lett.* **84** 5102 (2000)
85. Brabec T, Krausz F *Rev. Mod. Phys.* **72** 545 (2000)
86. Kan C, Burnett N H, Capjack C E, Rankin R *Phys. Rev. Lett.* **79** 2971 (1997)
87. Telle H R, Steinmeyer G, Dunlop A E, Stenger J, Sutter D H, Keller U *Appl. Phys. B* **69** 327 (1999)
88. Reichert J, Holzwarth R, Udem Th, Hänsch T W *Opt. Commun.* **172** 59 (1999)
89. Krausz F, Fermann M E, Brabec T, Curley P F, Hofer M, Ober M H, Spielmann C, Wintner E, Schidt A J *IEEE J. Quantum Electron.* **28** 2097 (1992)
90. Spielmann C, Curley P F, Brabec T, Krausz F *IEEE J. Quantum Electron.* **30** 1100 (1994)
91. Herrmann J *J. Opt. Soc. Am. B* **11** 498 (1994)
92. Magni V, Cerullo G, DeSilvestri S, Monguzzi A. *J. Opt. Soc. Am. B* **12** 476 (1995)
93. Kalashnikov V L, Kalosha V P, Poloiko I G, Mikhailov V P *Kvantovaya Elektron.* **24** 137 (1997)
94. Read K, Blonigen F, Ricelli N, Murnane M, Kapteyn H *Opt. Lett.* **21** 489 (1993)
95. Poppe A, Xu I, Krausz F, Spielmann C *IEEE J. Sel. Top.* **4** 179 (1998)
96. Asaki M T, Huang C-P, Garvey D, Zhou J, Kapteyn H C, Murnane M N *Opt. Lett.* **18** 977 (1993)
97. Szipöcz R, Ferencz K, Spielmann C, Krausz F *Opt. Lett.* **19** 201 (1994)
98. Pshenichnikov M S, de Boeij W P, Wiersma D A *Opt. Lett.* **19** 572 (1994)
99. Kryukov I V, Kryukov P G, Khoroshilov E V, Sharkov A V *Kvantovaya Elektron.* **15** 1320 (1988) [*Quantum Electron.* **18** 830 (1988)]
100. Martinez O E, Gordon J P, Fork R L *J. Opt. Soc. Am. A* **1** 1003 (1984)
101. Andreev A L, Mak A A, Yashin V E *Kvantovaya Elektron.* **24** 99 (1997) [*Quantum Electron.* **27** 95 (1997)]
102. Borodin V G, Komarov V M, Milinov V A, Mitel' V N, Nikitin N V, Popov V S, Potapov S L, Charukhchev A V, Chernov V N *Kvantovaya Elektron.* **29** 101 (1999) [*Quantum Electron.* **29** 939 (1999)]
103. Zeek E, Bartels R, Murnane M N, Kapteyan H C, Backus S *Opt. Lett.* **25** 587 (2000)
104. Albert O, Wang H, Liu D, Chang Z, Mourou G *Opt. Lett.* **25** 1125 (2000)
105. Sergeev A M, Gelikonov G V, Feldstein F I, Gladkova N D, Kamensky V A *OSA Tops* **2** 196 (1996)
106. Niering M, Holzwarth R, Reichert J, Pokasov P, Udem Th, Weitz M, Hansch T W, Lemonde P, Santarelli G, Abgrall M, Laurent P, Salomon C, Clainon A *Phys. Rev. Lett.* **84** 5496 (2000)
107. Birks T A, Wadsworth W J, Russell P St J *Opt. Lett.* **25** 1415 (2000)
108. Baklanov E V, Chebotaev V P, Dubetskiy B V *Appl. Phys.* **9** 171 (1976); Baklanov E V, Chebotaev V P *Kvantovaya Elektron.* **4** 2189 (1977) [*Quantum Electron.* **4** 1252 (1977)]
109. Liu X, Du D, Mourou G *IEEE Quantum Electron.* **38** 1706 (1997); Momma C, Nolte S, Kamlage G, von Alvensleben F, Tünnermann A *Appl. Phys. A* **67** 517 (1998)
110. Aus der Au J, Spuhler G J, Sudmeyer T, Paschotta R, Hövel R, Moser M, Erhard S, Karsiewski M, Giesen A, Keller U *Opt. Lett.* **25** 859 (2000)
111. L'Huillier A, Balcou P *Phys. Rev. Lett.* **70** 774 (1993)
112. Platonenko V T, Strelkov V V *Kvantovaya Elektron.* **25** 582 (1998) [*Quantum Electron.* **28** 564 (1998)]
113. Apolonski A, Poppe A, Tempea G, Spielmann Ch, Udem Th, Holzwarth R, Hänsch T W, Krausz F *Phys. Rev. Lett* **85** 740 (2000)
114. Papadogiannis N A, Witzel B, Kalpouzos C, Charalambidis D *Phys. Rev. Lett.* **83** 4289 (2000)
115. Chang Z, Rundqnist A, Wang H, Murnane M N, Kapteyn H C *Phys. Rev. Lett.* **79** 2967 (1997)
116. Bula C, McDonald K T, Prebys E J, Bamber C, Boege S, Kotseroglou T, Melissinos A C, Meyerhofer D D, Ragg W, Burke D L, Field R C, Horton-Smith G, Odian A C, Spencer J E, Walz D, Berridge S C, Bugg W M, Shmakov K, Weidemann A W *Phys. Rev. Lett.* **76** 3116 (1996)
117. Burke D L, Field R C, Horton-Smith G, Kotseroglou T, Walz D, Berridge S C, Bugg W M, Shmakov K, Weidemann A W, Bula C, McDonald K T, Prebys E J, Bamber C, Boege S J, Koffas T, Melissinos A C, Meyerhofer D D, Reis D A, Ragg W *Phys. Rev. Lett.* **79** 1626 (1997)
118. Pukhov A, Sheng Z-M, Meyerter Yehn J *Phys. Plasmas* **6** 2847 (1999)

119. Boyer K, Luk T S, Rhodes C K *Phys. Rev. Lett.* **60** 557 (1988)
120. Ledingham K W D, Spencer I, McCanny T, Singhal R P, Santala M I K, Clark E, Watts I, Beg E N, Zepf M, Krushelnick K, Tatarakis M, Danger A E, Norrey P A, Allott R, Neely D, Clark R J, Machacek A C, Wark J S, Cresswell A J, Sanderson D C W, Magill J *Phys. Rev. Lett.* **84** 899 (2000)
121. Cowan T E, Hunt A W, Phillips T W, Wilks S C, Perry M D, Brown C, Fountain W, Hatchett S, Johnson J, Key M H, Parnell T, Pennington D M, Snavely R A, Takahashi Y *Phys. Rev. Lett.* **84** 903 (2000)
122. Tabak M, Hammer J, Glinsky M E, Kruer W L, Wilks S C, Woodworlz J, Campbell E M, Perry M D *Phys. Plasmas* **1** 1626 (1994)
123. Kitagawa Y, Mima K, Azechi H, Takabe H, Nakai S, Yamanaka C in: *Research trends in physics, inertial confinement fussion* (K.A. Brueckner, ed.) (New York, AIP, 1992)
124. Perry M D, Mourou G *Science* **264** 917 (1994)